universität wien

MASTERARBEIT

„Identification and characterization of vitamin D target genes in human monocytes and macrophages“

verfasst von

Julia Wilfinger, Bakk

angestrebter akademischer Grad

Master of Science (MSc)

Wien, 2014

Studienkennzahl lt. Studienblatt:	A 066 838
Studienrichtung lt. Studienblatt:	Masterstudium Ernährungswissenschaften
Betreut von:	Carsten Carlberg, PhD, Professor of Biochemistry

Acknowledgement

I am deeply grateful to many people who gave me the possibility to complete this thesis. I want to thank the Institute of Biomedicine at the University of Eastern Finland in Kuopio for giving me permission to commence this thesis in first instance. I would like to express my special appreciation and acknowledgement to professor Carsten Carlberg for excellent guidance, caring and patience. I have been extremely lucky to have a supervisor who responded to my questions and queries so promptly. I would also like to thank all of the members of the Carlberg research group, especially Dr. Sabine Seuter for the practical support, cell culturing and friendship.

Special acknowledgement belongs to my family and friends for their unconditional support and encouragement during this period.

Vienna 2014

Julia Wilfinger

Abbreviations

$1,25(OH)_2D_3$ or 1,25D	1α,25-dihydroxyvitamin D_3
$25(OH)D_3$	25-dihydroxyvitamin D_3
B2M	beta-2-microglobulin
BMI	body mass index
bp	base pairs
CD14	CD14 molecule
CD97	CD97 molecule
cDNA	complementary deoxyribonucleic acid
ChIA-PET	chromatin interaction analysis with paired end tag sequencing
ChIP	chromatin immunoprecipitation
ChIP-seq	ChIP sequencing
CoA	co-activator proteins
CoR	co-repressor proteins
CP24A	$1,25(OH)_2D_3$ 24-hydroxylase
CTCF	CCCTC-binding factor
CYP24	25-hydroxyvitamin D-24-hydroxylase
CYP27B1	cytochrome p450, subgroup 27B1
DAF	decay accelerating factor
DBD	DNA-binding domain
DBP	vitamin D binding protein
DNA	deoxyribonucleic acid
DR3	direct repeat spaced by 3 nucleotides
EFSA	European Food Safety Authority
EGF	epidermal growth factor
FAIRE	formaldehyde-assisted isolation of regulatory elements
FAIRE-seq	formaldehyde-assisted isolation of regulatory elements sequencing
GAPDH	glycerinaldehyde-3-phosphate-dehydrogenase
HAT	histone acetyltransferase

HDAC	histone deacetylase
HDM	histone demethylase
HMT	histone methyltransferase
HPRT1	hypoxanthine phosphoribosyltransferase 1
IFN-γ	interferon-γ
IgG	immunoglobulin G
IGV	Integrative Genomics Viewer
IL	interleukin
IU	international unit
kb	kilo bases
LBD	ligand-binding domain
LRR	leucine rich repeats
LRRC8A	leucine rich repeat containing 8 family, member A
MB	myoglobin
mRNA	messenger ribonucleic acid
NOAEL	no observed adverse effect level
NRIP1	nuclear receptor interacting protein 1
PBMC	peripheral blood mononuclear cell
PBS	phosphate buffered saline
PMA	phorbol 12-myristate 13-acetate
PTH	parathyroid hormone
qPCR	real-time quantitative polymerase chain reaction
RANKL	nuclear factor-κB ligand
RE	response elements
RNA	ribonucleic acid
RNase	ribonuclease
RXR	retinoid X receptor
SLC37A2	solute carrier family 37, member 2
SP100	SP100 nuclear antigen
THBD	thrombomodulin
TLR	toll-like receptor

TNFα	tumor necrosis factor-
TSS	transcription start site
UL	tolerable upper intake level
VDR	vitamin D receptor

Table of contents

List of Figures

List of Tables

I Abstract

Vitamin D_3 belongs to the few nutritional compounds that has, via the binding of its metabolite 1α,25-dihydroxyvitamin D_3 ($1,25(OH)_2D_3$) to the transcription factor vitamin D receptor (VDR), a direct effect on gene regulation. The relation of thousands of genomic VDR binding sites to a few hundred primary $1,25(OH)_2D_3$ target genes is still largely unresolved. We studied chromatin domains containing genes for the adhesion molecules CD97 and LRRC8A, the glucose transporter SLC37A2 and the co-activator NRIP1. These domains vary significantly in size (7.3 to 956 kilo bases (kb)) but contain each one major VDR binding site. In monocytic cells these four sites are associated with open chromatin and occupied by VDR, while in macrophage-like cells only the sites of *LRRC8A*, *SLC37A2* and *NRIP1* are accessible and receptor-bound. The VDR site of *CD97* does, in contrast to the three other loci, not carry any direct repeat spaced by 3 nucleotides (DR3)-type binding sequence. *CD97*, *LRRC8A*, *SLC37A2* and *NRIP1* are early responding $1,25(OH)_2D_3$ target genes in monocytic cells, while in macrophage-like cells they respond less and in part delayed. In primary human peripheral blood mononuclear (PBMC) cells from 71 pre-diabetic subjects of a vitamin D_3 intervention study (VitDmet) *CD97*, *LRRC8A*, *SLC37A2* and *NRIP1* can be used as transcriptomic biomarkers for classifying human individuals for their possible benefit from vitamin D_3 supplementation. In particular, *NRIP1* exceeds the potential of the previously identified marker *CD14* by more than 40% and seems to be a well-suited molecular marker for the vitamin D status in the hematopoietic system.

II Literature survey

II.I Vitamin D

Vitamin D is a fat-soluble vitamin and plays a special role among the vitamins, because it can be synthesized in the skin upon exposure to UV-B radiation and it can be obtained from the diet. This makes it challenging to develop dietary reference intake recommendations. Vitamin D_3 sources are cod liver oil, egg yolk and fatty fish like salmon, mackerel and tuna and vitamin D_3 fortified food like margarine, milk or bread. Vitamin D occurs in two forms, vitamin D_3 (also called cholecalciferol) is derived from animals and vitamin D_2 (also called ergocalciferol) is isolated from plants[1,2,1].

II.II Absorption of vitamin D

Vitamin D is absorbed with fat and transported from the intestine in chylomicrons via the lymphatic system. Therefore, the presence of fat in the lumen is necessary for releasing bile acid and pancreatic lipase. Bile acid assists the formation of lipid-contained micelles, which diffuse into enterocytes. From there vitamin D is packed with other lipophilic molecules into chylomicrons and reaches the systemic circulation via the lymphatic system. The absorption rate is about 80%[3,1].

[1] Deutsche Gesellschaft für Ernährung, Österreichische Gesellschaft für Ernährung, Schweizerische Gesellschaft für Ernährungsforschung, Schweizerische Vereinigung für Ernährung. Referenzwerte für die Nährstoffzufuhr Vitamin D. Neuer Umschau Buchverlag. 1. Auflage, 4. Korrigierter Nachdruck. 2012.
[2] Higdon J. Linus Pauling Institute. Oregon State University. Last updated 6/22/11. http://lpi.oregonstate.edu/infocenter/vitamins/vitaminD/. (October 2013).
[3] Shils M, Shike M, Ross A C et al. Modern nutrition in health and disease. Lippincott Williams & Wilkins, USA, 10. edition (2006).

II.III Synthesis in the skin

7-dehydrocholesterol is the natural precursor of vitamin D_3. For the transformation of 7-dehydrocholesterol into vitamin D_3 a UV-B radiation with the wavelength of 280-320 nm is needed[2].

The production of vitamin D_3 in the skin depends on the duration of the UVB-exposure, the season of the year, the latitude, the age, as well as the surface of the skin, the use of sun cream, clothing and the pigmentation of the skin[1,3].

The synthesis of vitamin D_3 in the skin contributes to 80–90% to the vitamin D supply in humans. This is based on the fact that in healthy young adults the circulating 25-hydroxyvitamin D_3 ($25(OH)D_3$) concentration lies between 30-80 nM [4] and 1 µg vitamin D_3 (for example, obtained from a supplementation) increases the circulating $25(OH)D_3$ concentration by only about 1-3 nM[5,6]. The dietary vitamin D intake is below 5 µg[7] per day and therefore doesn't have a big effect on the $25(OH)D_3$ serum concentration either[4].

II.IV Storage of vitamin D

Adipose tissue is the major storage location for vitamin D, because of its hydrophobic nature it has a low rate of release[1,8]. For that reason obese people may need larger doses of vitamin D supplements to achieve a defined serum level than average weight people[1].

II.V Activation of vitamin D

Vitamin D, synthesized in the skin or consumed with food, itself is biologically inactive and has to be metabolized to its biologically active forms. Therefore, it goes via the blood circulation bound to a specific plasma carrier protein, vitamin D binding protein (DBP), first to the liver, where vitamin D is hydroxylated to $25(OH)D_3$. This is the major circulation form of vitamin D and

the $25(OH)D_3$ level is a useful indicator of the vitamin D nutritional status. It increases with higher sun exposure and the dietary intake of vitamin D. The second hydroxylation takes place mainly in the kidney by the enzyme 25-hydroxyvitamin-D_3-1-hydroxylase, also known as cytochrome p450 27B1 (CYP27B1). The result is the formation of $1,25(OH)_2D_3$ (also called calcitriol), which is the biologically most active form of vitamin D. Most of the physiological effects of vitamin D are directly related to effects of $1,25(OH)_2D_3$[4,5].
In addition to the kidney, some other $1,25(OH)_2D_3$ target organs are also able to produce $1,25(OH)_2D_3$[9] (see chapter II.VI.II Vitamin D and the immune system).

The plasma concentration and renal production of $1,25(OH)_2D_3$ are regulated by a feedback mechanism of the vitamin itself and by plasma parathyroid hormone (PTH) levels and serum calcium and phosphorus levels as well as the fibroblast growth factor 23. The enzyme 25-hydroxyvitamin D-24-hydroxylase (CYP24) catabolizes $25(OH)D_3$ and $1,25(OH)_2D_3$ into their biologically inactive and water-soluble form, calcitroic acid. This metabolism takes place in the kidney and calcitroic acid is the major end product excreted in the urine[10].

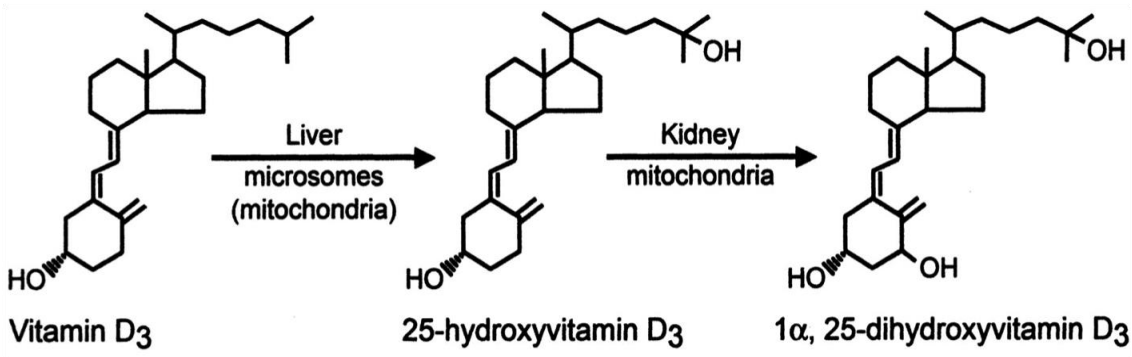

Figure 1: Metabolic activation of vitamin D_3 to its hormonal form, $1,25(OH)_2D_3$[11]

[4] Deutsche Gesellschaft für Ernährung, Österreichische Gesellschaft für Ernährung, Schweizerische Gesellschaft für Ernährungsforschung, Schweizerische Vereinigung für Ernährung. Referenzwerte für die Nährstoffzufuhr Vitamin D. Neuer Umschau Buchverlag. 1. Auflage, 4. Korrigierter Nachdruck. 2012.
[5] Higdon J. Linus Pauling Institute. Oregon State University. Last updated 6/22/11. http://lpi.oregonstate.edu/infocenter/vitamins/vitaminD/. (October 2013).

II.VI Functions

During the studies of rickets in the early 20th century scientists discovered and described the “sun” vitamin D[6]. Since then the interaction of bone calcification and vitamin D was established and professionals thought the major health problem resulting from vitamin D deficiency are rickets, osteomalacia and osteoporosis. However, these bone diseases can be considered as the tip of the vitamin D deficiency iceberg. In fact, vitamin D plays a major role relating to the increasing risk of many chronic illnesses, including common cancers, autoimmune diseases, infectious diseases and cardiovascular diseases[10].

II.VI.I Calcium balance

Maintenance of serum calcium level within a fairly narrow range (from 8.5 to 10.5 mg/dl, normal values and reference ranges may vary among laboratories as much as 0.5 mg/dl)[7] are essential for normal functioning of the nervous system, bone growth and conservation of bone density. For the efficient absorption and utilization of calcium by the body, vitamin D is also needed[12]. The parathyroid glands sense low serum calcium levels by G protein coupled transmembrane receptors and secrete PTH. Boosts in PTH increase the activity of the enzyme CYP27B1 in the kidney and thus the production of $1,25(OH)_2D_3$. These elevations result in changes in gene expression that normalize serum calcium levels by i) raising the intestinal absorption of dietary calcium, ii) increasing the reabsorption of calcium in the kidneys and iii) mobilizing calcium from the bone depot when there is insufficient dietary calcium to maintain normal serum levels[8,11].

[6] Chick H, Dolyell E J, Hume E M. Studies of rickets in Vienna 1919-1922. Medical Research Council. 1923.
[7] Walker H K, Hall W D, Hurst J W. Clincial Methods, 3rd edition The History, Physical and Laboratory Examinatons. Emory University School of Medicine. Atlanta. 1990.
[8] Higdon J. Linus Pauling Institute. Oregon State University. Last updated 6/22/11. http://lpi.oregonstate.edu/infocenter/vitamins/vitaminD/. (October 2013).

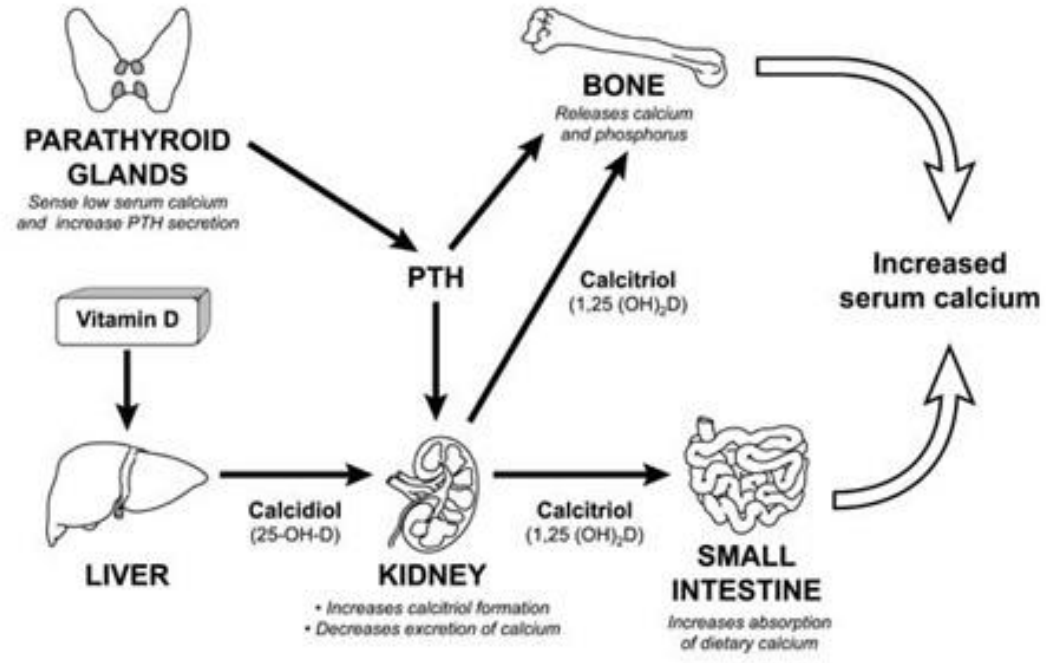

Figure 2: The parathyroid glands sense the serum calcium level and secrete PTH, if it becomes too low. PTH stimulates the activity of the enzyme CYP27B1 in the kidney, resulting in increased production of $1,25(OH)_2D_3$. Increased $1,25(OH)_2D_3$ production restores normal serum calcium levels in three different ways: 1) by activating the vitamin D-dependent transport system in the small intestine, increasing the absorption of dietary calcium; 2) by increasing the mobilization of calcium from bone into the circulation; and 3) by increasing the reabsorption of calcium by the kidneys. PTH is also required to increase calcium mobilization from bone and calcium reabsorption by the kidneys. However, PTH is not required for the effect of $1,25(OH)_2D_3$ on the intestinal absorption of calcium[9].

Two mechanisms play a role in increasing serum calcium levels, when no intestinal calcium absorption is contingent. First, the distal renal tubule is responsible for reabsorption of calcium and vitamin D as well as PTH is involved in this process. Vitamin D_3 stimulates enterocytes to absorb calcium and phosphate. When the plasma calcium level fails to respond, the parathyroid glands secrete PTH, which increases the production of vitamin D_3 to mobilize bone calcium[11].

Secondly, vitamin D_3 stimulates osteoblasts to produce receptor activator nuclear factor-κB ligand (RANKL), which stimulates osteoclastogenesis and

[9] Higdon J. Linus Pauling Institute. Oregon State University. Last updated 6/22/11. http://lpi.oregonstate.edu/infocenter/vitamins/vitaminD/. (October 2013).

activates resting osteoclasts for bone resorption. PTH is also required for this mobilization event. Under normal conditions environmental calcium is used first and only in its absence the internal stores are used[11].

When the serum calcium concentration rises, the C-cells of the thyroid gland secrete the 32-amino acid peptide calcitonin. This peptide blocks bone calcium mobilization and stimulates the renal 1α-hydroxylase to provide vitamin D for non-calcemic needs[11].

II.VI.II Vitamin D and the immune system

The link between vitamin D and immune functions was assured with the finding, that children with nutritional rickets were more likely to experience infections of the respiratory system[13].

$1,25(OH)_2D_3$ stimulates the differentiation of monocytes into mature macrophages. The innate immune system is activated as well, while having an inhibitory effect on the adaptive immune response[9,14].

After toll-like receptor (TLR) activation of human macrophages by pathogens, VDR and CYP27B1 expression is increased. Mitochondrial CYP27B1 converts $25(OH)D_3$ to $1,25(OH)_2D_3$ in macrophages and the latter binds to VDR and leads to the induction of the anti-microbial peptide cathelicidin. Therefore, vitamin D is a key link between TLR activation and innate cellular anti-bacterial response[15,16].

Macrophage $1,25(OH)_2D_3$ synthesis can also function as negative auto-regulation via the increased expression of the feedback enzyme CYP24 and via down-regulation of TLR expression. Besides macrophage CYP27B1 might also induce paracrine responses by $1,25(OH)_2D_3$ secretion in monocytes and T or B lymphocytes (see Figure 3)[16,17].

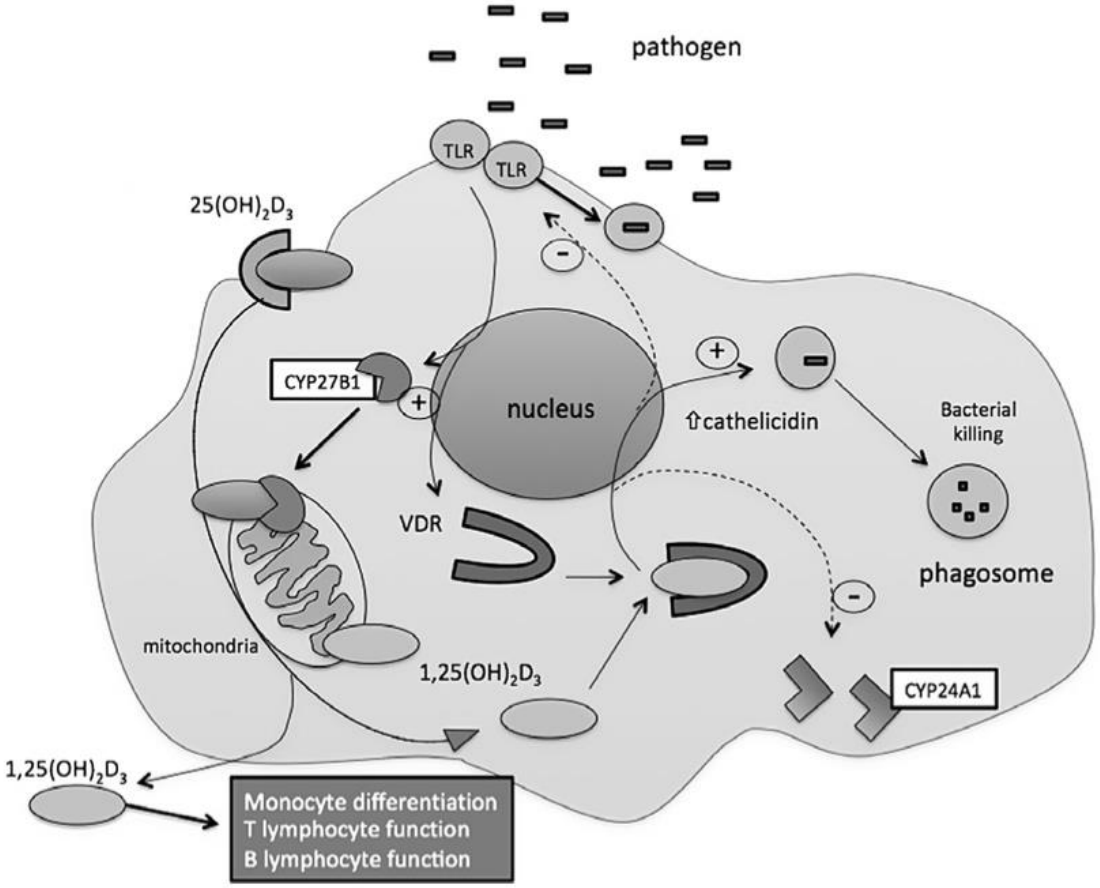

Figure 3: Vitamin D and innate immunity. Activation of macrophage TLR signaling by pathogens results in the transcriptional induction of *VDR* and expression of CYP27B1. Circulating $25(OH)D_3$ enters macrophages and is converted to $1,25(OH)_2D_3$ by mitochondrial CYP27B1, which can bind to the VDR in the cell. Once bound to VDR, $1,25(OH)_2D_3$ is able to act as a transcription factor leading to the induction of cathelicidin expression. Incorporation into phagosomes containing an internalized pathogen enables cathelicidin to function as an antibacterial agent. As well as up-regulating cathelicidin expression, macrophage synthesis of $1,25(OH)_2D_3$ can also facilitate negative autoregulation by increased expression of the feedback enzyme CYP24 and by downregulation of TLR expression. In parallel with autocrine effects on innate antibacterial function, macrophage CYP27B1 may also induce paracrine responses in monocytes and T or B cells as a consequence of $1,25(OH)_2D_3$ secretion[16,17].

Vitamin D also influences antigen presentation and thus plays a key role between the innate and adaptive immune system. $1,25(OH)_2D_3$ is able to regulate the proliferation and function of macrophages, dendritic cells and activated T and B cells via VDR and CYP27B1 expression.

$1,25(OH)_2D_3$ suppresses the production of immunoglobulin by human PBMCs and maturation of dendritic cells decreases by inhibiting expression of co-

stimulatory molecules. Thus, the ability to present antigens is reduced and also the activation of T cells[17].

Immune activity of CYP27B1 is controlled by cytokine exposure, such as tumor necrosis factor-α (TNFα), interferon-γ (IFNγ) and interleukins (IL) 1 and 2[17].

II.VII Cells of the immune system

The innate immune system acts as the first line of host defense against pathogens and represents diverse cellular components like granulocytes, mast cells, monocytes, macrophages, dendritic cells and natural killer cells[18].

II.VII.I Monocytes

Monocytes incorporate about 5-10% of peripheral blood leukocytes in humans and they develop from a myeloid precursor in the bone marrow. After release into the circulation they enter tissues where they are collectively called macrophages[19]. The half-life of these cells in human blood is with 1-3 days rather short and their morphological features are an irregular shape, a high cytoplasm-to-nucleus ratio and a light blue cytoplasm[19,20]. Monocytes are able to differentiate into macrophages or dendritic cells. Thus, the short half-life support the belief that blood monocytes continuously repopulate macrophage and dendritic cell populations to maintain homeostasis and control innate and adaptive immunity[18,20]. Monocytes show heterogeneity by different expression of CD14 (part of the receptor for lipopolysaccharide) and CD16 and chemokine receptors. The so-called “classic” $CD14^{+}CD16^{-}$ subset represents 95% of the monocytes in a healthy individual whereas the “non-classical” $Cd14^{low}CD16^{+}$ monocytes contain the remaining fraction of monocytes. It seems that among the CD16 monocytes an “intermediate” population exists, which is $CD14^{+}CD16^{+}$ [20].

II.VII.II Macrophages

Macrophages arise from monocytes and are found in all tissues where they illustrate a huge anatomic and functional diversity. Specialized tissue macrophages are osteoclasts in bone, alveolar macrophages in the lung, histiocytes in the interstitial connective tissue and Kupffer cells in the liver[21]. These cells play a role in development, homeostasis, repair and immune response. Macrophages are, as monocytes, heterogeneous and can rapidly change their function due to local micro environmental signals. For example IFNγ in combination with lipopolysaccharide (LPS) induces the classically activated M1 macrophages, whereas IL-4 and IL-13 stimulate the alternatively activated M2 macrophages[18]. M1 macrophages have a role in antitumor immunity as well as defense of the host from a variety of bacteria, protozoa and viruses, in contrast M2 macrophages mediate wound healing and have anti-inflammatory functions[21].

II.VII.III Human peripheral blood mononuclear cells

Human PBMCs include lymphocytes and monocytes and can be collected easily, repeatedly and with minimum invasion. They travel through the body and reflect gene expression changes due to different tissues in response to internal or external stimuli and are useful for nutritional studies, showing specific effects of diets or nutrients[22]. Gene expression profiles of PBMCs have been proven to be highly robust in distinguishing a disease from a healthy state and therefore they are representing an attractive tissue source in clinical pharmacogenomic studies[23].

II.VIII Gene expression

The nucleus is arranged into chromosome areas and they are divided into genomic domains. The basic types of genetic information are triplets of bases, which encode for different amino acids[24].

Gene expression includes several steps from the zygotic genome to the final polypeptide and is controlled by regulative factors. The first step in gene expression is the organization of chromatin in the nucleus into chromosomal territories with a following activation. During transcription pre-messenger ribonucleic acid (pre-mRNA) is synthetized, mediated by RNA polymerase 2. Pre-mRNA includes exons of a single coding sequence and associates with nuclear RNA-binding proteins, resulting in pre-messenger ribonucleoproteins (pre-mRNPs). Pre-mRNAs are stored in the nucleus, degraded or selected for productive splicing. For that reason it presents the major regulative process in gene expression. After processing, splicing and formation of mRNP, mRNA gets transported in the cytoplasm. Cytoplasmic inactive mRNPs are formed and nuclear RNP-type proteins are replaced with cytoplasmic ones and accordingly mRNP proteins by translation factors. Cytoplasmic mRNA repression is a crucial step of control of selective gene expression, occurs to be reversible and furthermore mRNAs may shuttle between the active and repressed states. The two ribosome-units associate into functional ribosomes and translation of the coding sequence in mRNA takes place. Primary polypeptides are formed with folding into its secondary protein structure. The post-translational process of gene expression includes the formation of tertiary and quaternary protein structures and is controlled by homeostasis of protein biosynthesis and degradation[25,26].

Cis- and transacting receptors represent a program that generates the gene within a given cellular space and time. Cis-acting receptors are located in the same strand of deoxyribonucleic acid (DNA) or ribonucleic acid (RNA), whereas trans-acting receptors are in the milieu and act on the signals placed in cis and regulate the process between transcription and translation[24].

Taken together gene expression results in the synthesis of proteins or RNA, which carry out a given structural or enzymatic function. According to these, protein genes and RNA genes exist, as well as structural genes and controlling genes[24].

Regulation of gene expression operates mainly by association of regulatory protein and interfering RNAs as well as by the action of the enzymes involved in the transcription and processing machinery[24,25]. Furthermore gene regulation is a complex process because numerous factors appear to be required for the temporal and areal regulation of genes. These factors are implanting into multi-protein complexes and contribute to specific gene regulation events. One of the most useful techniques for understanding this level of gene regulation is the Chromatin Immunoprecipitation assay (ChIP)[27] (for more details see chapter Chromatin Immunoprecipitation).

II.IX Chromatin

The human genome consists of 3.26×10^9 base pairs (bp), which represents a length of 2 m. Since cell nuclei are as small as 10 µm in diameter, the long genomic DNA has to be significantly compacted in the form of chromatin[**10,11**].

Histones are primary positively charged proteins, which mediate the folding of negatively charged genomic DNA into the repeating units of nucleosomes that form chromatin. Each nucleosome contains two copies of the four histone proteins H2A, H2B, H3 and H4. The DNA is wrapped around these histone octamers. Multiple variant histone proteins can replace conventional ones and influence the overall chromatin structure to support expression or suppression of genes[**10,11**,28].

The N-termini of specific arginine, serine or lysine residues of the histones H2A, H2B, H3 and H4 is able to interact with phosphate-, methyl-, and acetyl groups and consequently influence the folding and functional state of the chromatin fiber[**11**,28].

[**10**] Wolffe A. Chapter two – Chromatin Structure. Chromatin (Third Edition). 1998. Pages 7-172.
[**11**] Gordon J. A. R, Grandy R. A, Lian J. B, Stein J. L, van Wijnen A. J, Stein G. S. Chromatin. University of Massachusetts Medical School. USA. 2013.

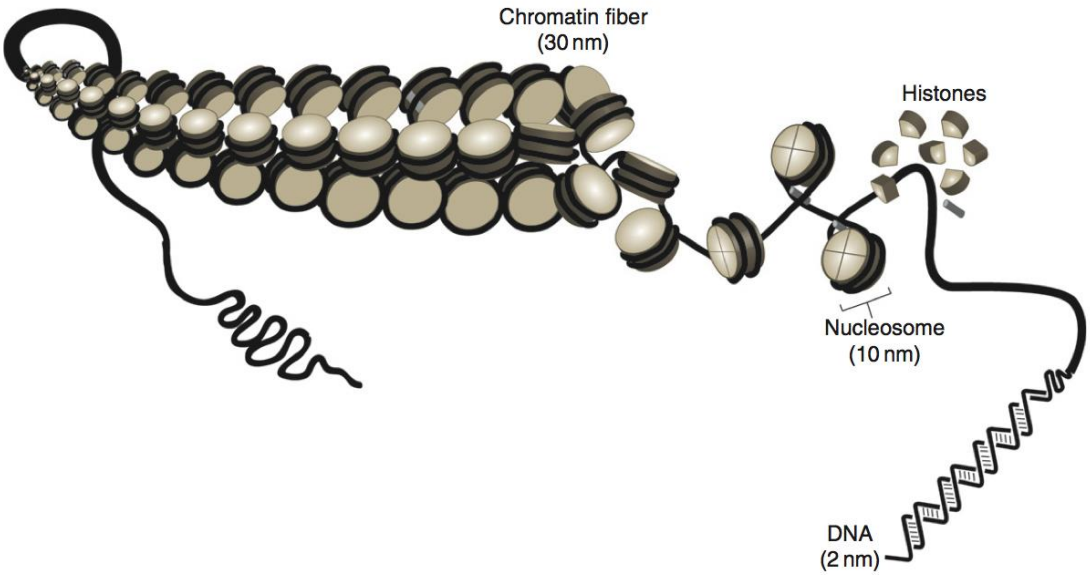

Figure 4: Model of chromatin packing into higher order structures. DNA is wrapped around histone octamers to form nucleosomes[12].

Chromatin structure plays a significant role in gene regulation by an enriched histone acetylation and accessible chromatin conformation of active genes and the association of nucleosome-free regions and gene regulatory elements[29]. Thus for gene expression the condensed genomic DNA has to remodel its structure to be accessible for the regulatory transcription machinery. Many chromatin-associated proteins, like transcription factors, require histone-free DNA for binding[30]. On the other hand is open chromatin associated with all known classes of active DNA regulatory elements including promoters, enhancers, silencers, isolators and locus control regions[31].

Formaldehyde Assisted Isolation of Regulatory Elements sequencing (FAIRE-seq) can be used to generate genome-wide open chromatin maps and identify assessable chromatin regions[31] (for more details see chapter Formaldehyde Assisted Isolation of Regulatory Elements).

[12] Gordon J. A. R, Grandy R. A, Lian J. B, Stein J. L, van Wijnen A. J, Stein G. S. Chromatin. University of Massachusetts Medical School. USA. 2013.

II.X Chromatin immunoprecipitation

The ChIP method is used for detailed analysis of enhancer and promoter regions of primary transcription factor target genes in living cells. In any chosen time point nuclear proteins can be fixed with mild chemical cross-linking to genomic DNA in living cells or tissues. After sonication of chromatin into fragments in size of 200-400 bp, immunoprecipitation with an antibody against the chosen nuclear protein is performed. Thereby chromatin regions that had been in contact with the protein of choice, for example VDR, at the moment of cross-linking, are enriched. After a reverse cross-linking reaction, the chromatin fragments are obtained, which represent the subset of the genome, which had been in contact with the protein of choice. The chromatin fragments can be tested for a few selected regions, by using quantitative polymerase chain reaction (qPCR) using primers specific for the chosen genomic region (ChIP-qPCR), or subjected to massive parallel sequencing (ChIP-seq) to obtain genome-wide binding data. An indication for a nuclear protein-DNA binding for a given genomic region is the observation of a significant enrichment in relation to a control, which can be generated by using unspecific immunoglobulins (IgGs) for the immunoprecipitation[27,32].

II.XI Formaldehyde Assisted Isolation of Regulatory Elements

Chromatin stability and consequently DNA regulating processes like transcription are governed by a combination of factors acting together and result in a context-specific set of DNA elements bound by regulatory factors. The method Formaldehyde Assisted Isolation of Regulatory Elements (FAIRE) is a strategy to isolate and map genomic regions depleted of nucleosomes, such as active transcription start sites (TSS) and accessible transcription factor binding sites. One prerequisite for this method is the higher efficiency of crosslinking of histone proteins to DNA than the efficiency of sequence-specific proteins to DNA. This difference is likely due to formaldehyde’s short crosslinking distance and crosslinks are only formed between proteins and DNA in direct contact.

Another factor is the needed ε-amino group for formaldehyde to form a crosslink. Such amino groups occur on lysines and about 10% of the amino-acid composition of histones are lysines. This is a much higher proportion than in a typical protein[33].

The assay includes crosslinking of histones to DNA, shearing the chromatin by sonication, performing a phenol-chloroform extraction and mapping the genomic region by next-generation DNA sequencing. Protein-free DNA (blue fragments, Figure 5) remains in the aqueous phase and is isolated, while nucleosome bound DNA (black fragments, Figure 5) persists in the phenol phase. The reference or input chromatin is not cross-linked and represents the total DNA of the cells. qPCR can be used to assay specific loci to screen many cell or tissue types[33] (see Figure 5).

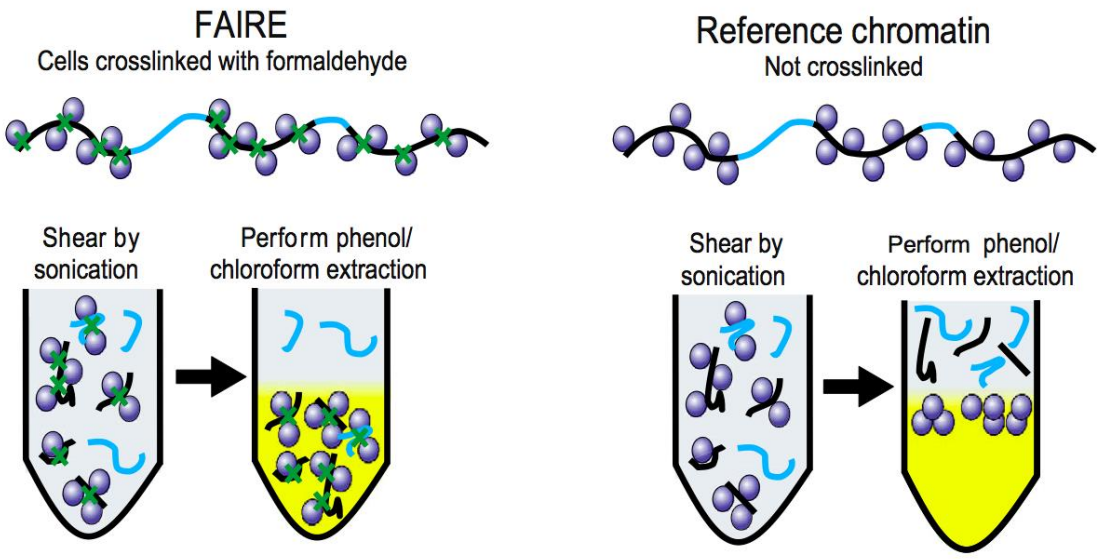

Figure 5: FAIRE assay. The FAIRE procedure is shown on the left, while preparation of the reference or input sample is shown on the right. The DNA recovered from the aqueous phase of each extraction can then be used to identify sites of open chromatin using qPCR or high-throughput sequencing applications[33].

II.XII ChIA-PET

Chromatin Interaction Analysis by Paired-End Tag Sequencing (ChIA-PET) is a technique that incorporates ChIP-based enrichment, chromatin proximity ligation, paired-end tags and high-throughput sequencing to determine *de novo* long-range chromatin interactions genome-wide. The principle in short: crosslinked chromatin interaction nodes are bound by proteins and are enriched by ChIP. Remote DNA elements tethered together in close spatial distance are connected through ligation with oligonucleotide DNA linkers. The paired-end tag (PET) construct contains a 20 bp head tag, a 38 bp linker sequence and a 20 bp tail tag. This is the template for next generation paired-end sequencing and after mapping to the corresponding reference genome the genomic distance between two tags will be analyzed. They show, whether a PET is derived from a self-ligation product of a single DNA fragment or an inter-ligation product of two DNA fragments. Singletons mostly reflect random background noise and overlapping ChIP fragments indicate true binding sites and long-range chromatin[34].

The ChIA-PET assay generates two types of datasets, the binding sites defined by ChIP enrichment and the interactions between two binding loci illustrated by ligation events. According to previous publications, ChIA-PET is an adequate method to characterize transcription factors in a global chromatin organization[35].

Sequences bound by CCCTC-binding factor (CTCF) divide transcriptional and chromatin domains and are highly conserved from fly to human[36]. CTCF sites function as genome organizer and therefore create local chromatin hubs and clusters of genes with coordinate expression, facilitate communication between regulatory elements and promoters and demarcate boundaries between chromatin and sub-nuclear compartments[35]. The ChIA-PET method has been successfully used to provide insights into the CTCF-associated global chromatin organization[35].

II.XIII VDR

VDR is one of the approximately 1900 classical transcription factors, which are encoded by the human genome. Transcription factors control gene expression and their action regulates cell function and they respond to the environment[32,37]. VDR belongs to the nuclear receptor superfamily of which most members are activated by small lipophilic molecules in the size and molecular weight of cholesterol. The members of this family contain a highly conserved DNA-binding domain (DBD) and a structurally conserved ligand-binding domain (LBD)[38].

Already low nanomolar concentrations of its ligand $1,25(OH)_2D_3$ can specifically activate VDR[39]. VDR ligand specificity is obtained through a limited number of stereo-specific polar contacts that include anchoring points and the shape of the ligand-binding pocket within its LBD. VDR binds its ligand with high affinity and has a relatively small ligand-binding pocket, which is filled to a high percentage by ligand[32,40].

VDR's DBD contacts six nucleotides within the major groove of genomic DNA. However, the DNA-binding affinity of monomeric VDR is insufficient for a stable protein-DNA complex formation. Therefore, a complex with a partner-protein is needed in order to achieve efficient DNA binding. The nuclear receptor retinoid X receptor (RXR) is the predominant partner of VDR[41].
Spaced hexameric binding motifs are needed for the dimerization of nuclear receptor DBDs and are referred to as response elements (RE). Asymmetric, direct repeat arrangements of two motifs spaced by three nucleotides, DR3, characterize such response elements and provide an efficient interface of the DBDs of VDR and RXR[32] (see Figure 6).

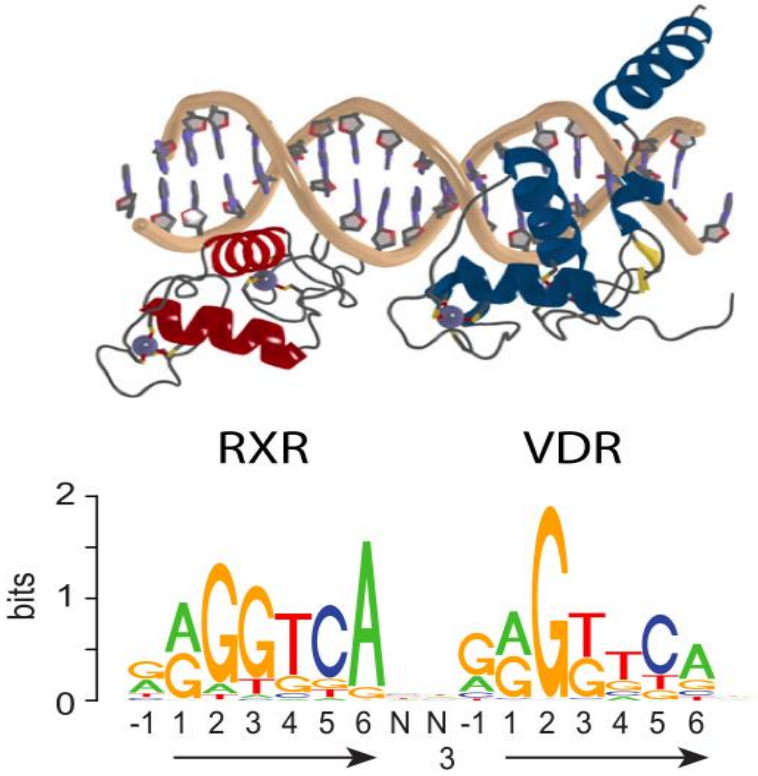

Figure 6: VDR binding sites. The crystal structure of the heterodimer of the DBDs of VDR (blue) and RXR (red) bound to a DR3-type RE (top) is aligned with the *de novo* DR3-type sequence motif[32].

Approximately one third of all genomic binding sites of VDR contain DR3-type REs. In order to explain the binding of VDR to non-DR3-type sequences other mechanisms must exist, how VDR associates with genomic loci and controls target genes. Two mechanisms are suggested, first partnering with presently undefined partner protein (see Figure 7, middle) and secondly the tethering to other DNA-binding transcription factors (see Figure 7, bottom)[32].

Co-activator proteins (CoA) stimulate the transcription of the target gene by building a bridge to the basal transcriptional machinery, which is assembled on the TSS of the primary VDR target gene. This process is referred to as transactivation[32].

VDR binding sites are found up- and downstream of the TSS region of the primary target genes and the likelihood of a functional VDR binding site decreases with increasing range from the TSS, however no maximal distance is known[32].

After ligand activation, the VDR most likely shifts from genomic regions without DR3-type RE to those with a DR3-type RE. Non-DR3 locations may serve as a nuclear store of VDR and can, after ligand binding, rapidly transport VDR into the nucleus[32].

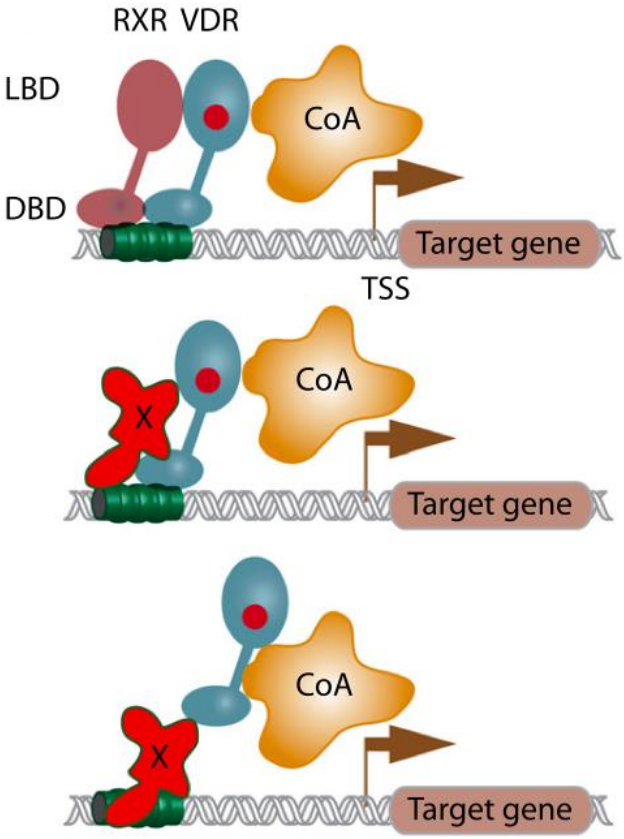

Figure 7: VDR binding sites. Three modes of VDR regulating its primary target genes are indicated: VDR–RXR heterodimers preferentially binding to a DR3-type RE (top), VDR partnering with undefined protein X bound to DNA (middle) and VDR tethering undefined protein X bound to DNA (bottom). In all three cases it is assumed that the contact of ligand (red)-activated VDR leads to an association with CoA proteins and the activation of primary target genes[32].

The VDR gene is highly expressed in kidney, bone and intestine tissue and at least low to moderately in nearly all other of the around 250 human tissues and cell types[42].

Even in the absence of the ligand 1,25$(OH)_2D_3$ VDR is able to bind its genomic target. Consequently, the functional profile of the VDR is larger than that of its ligand[43].

The epigenetic landscape leads to short-lived states, such as a response of chromatin to extra- and intracellular signals like an exposure of $1,25(OH)_2D_3$[44]. Epigenetic changes can be reversible post-translational modifications of histone proteins, such as acetylation and methylation. These are directed by chromatin modifying enzymes like histone acetyltransferases (HAT), histone deacetylases (HDAC), histone methyltransferases (HMT) or histone demethylases (HDM)[45].

In the deactivation phase the ligand is absent and VDR interacts with co-repressor proteins (CoR), which further associate with HDACs. That leads to compact chromatin-packing[46]. In the activation phase the ligand is present and induces the dissociation of CoRs and the association of CoAs[47,48]. CoAs can have HAT activity and consequently cause local chromatin relaxation[47]. VDR is also able to interact with another class of CoAs, which are members of the mediator complex. They build a bridge to the basal transcriptional machinery and initiate a burst of mRNA synthesis by RNA polymerase II. This process is called initiation phase (see Figure 8).

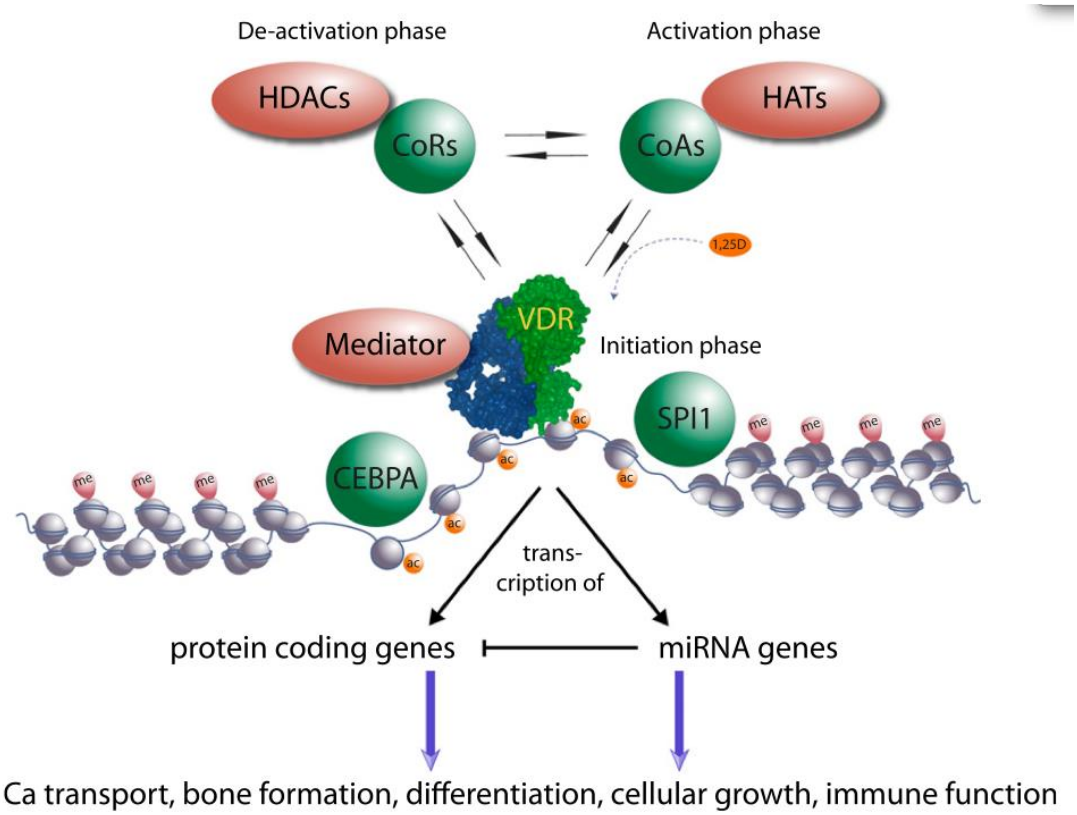

Figure 8: Integration of VDR actions. Together with the pioneering factors the VDR is the central part of a differentiation module. Putative pioneer factors such as CEBPA and SPI1 appear to help the VDR to access its genomic binding sites, but may not be found at all VDR binding loci. At these genomic VDR binding regions there is a cyclical alternation of proteins representing the deactivation phase (CoRs and HDACs), the activation phase (CoAs and HATs) and the initiation phase (VDR and Mediator proteins). The outcome of the dynamic interaction of VDR with its binding sites and partner proteins is the modulation of the transcription of its primary target genes. The latter are either protein coding genes or non-coding genes, such as miRNA genes. Some of the miRNAs are involved in the fine-tuning of the mRNA expression of the protein-coding genes. Together with secondary target genes they mediate the physiological actions of $1,25(OH)_2D_3$ and its receptor VDR[32].

II.XIII.I VDR ChIP-seq

Four VDR ChIP-seq studies have been published to date, in human lymphoblastoids[49], human monocytes (THP-1)[50], colorectal cells (LS180)[51] and hepatic stellate cells[52]. Human lymphoblastoids were treated for 36 h with $1,25(OH)_2D_3$ and 2776 genomic VDR-binding sites were reported. In human monocytes after 40 min ligand stimulation 1820 VDR ChIP-seq peaks were observed and 1171 only occur in the presence of $1,25(OH)_2D_3$. In the absence of ligand in lymphoblastoids and monocytes 623 and 520 VDR sites could be identified[32,49,50]. Colorectal cells (LS180) were stimulated for 180 min with $1,25(OH)_2D_3$ and 1674 VDR-binding sites co-locate with those of the VDR partner protein RXR were shown[51].

The four ChIP-seq studies revealed a comparable number of VDR-binding sites of about 1600-2700 specific peaks but only 20% of these sites are identical in human lymphoblastoids, THP-1 and LS180 cells. This confirms that most VDR target genes respond to $1,25(OH)_2D_3$ in a very tissue- and time-specific fashion[32].
Another interesting fact is, that the higher the fold enrichment of a VDR peak, the higher is the chance that it contains a high-quality DR3-type RE. Thus, this element plays an important role of VDR regulation[53].

In monocytes 408 genes out of 638 are up-regulated and approximately 70% of these peaks are in a range of 400 kb from the core promoter region. Only 99 down-regulated genes out of 230 have a $1,25(OH)_2D_3$-stimulated VDR peak

within 400 kb distance. Therefore, the down-regulation mechanism seems to be different from that of up-regulation[32].

The combination of ligand stimulation for VDR location mapping and mRNA expression analysis for the same cellular model allows a more detailed exploration of the mechanisms of VDR target gene regulation. The change of mRNA expression is a direct consequence of the binding of VDR to genomic regions looping to their respective core promoter region[32].

II.XIV Vitamin D supplementation

The D-A-CH (Germany, Austria, Switzerland) vitamin D recommendation for the daily intake is 20 μg, which corresponds to 800 international units (IU) (1 μg vitamin D = 40 IU), identified by the "Deutsche Gesellschaft für Ernährung". This estimated value includes dietary intake as well as endogen synthesis in the skin[13]. A consumption study in Germany (2008) indicated an average daily intake of vitamin D of 2,9 μg for men and 2.2 μg for women far below the recommendations, excluding endogenous synthesis[14]. Although the importance of the synthesis in the skin on the vitamin D status, which represents 80-90%, is known and well established, during winter time, people with less sun exposure, as well as people who are living in the northern hemisphere seem to be on special vitamin D deficiency risk[13]. Therefore the evaluation of the $25(OH)D_3$ serum level is more sensible. A Germany-wide measurement of $25(OH)D_3$ levels investigated that 57% of men and 58% of women have serum levels below the reference value 50 nmol/l (nM)[15]. For that reason vitamin D

[13] Deutsche Gesellschaft für Ernährung, Österreichische Gesellschaft für Ernährung, Schweizerische Gesellschaft für Ernährungsforschung, Schweizerische Vereinigung für Ernährung. Referenzwerte für die Nährstoffzufuhr Vitamin D. Neuer Umschau Buchverlag. 1. Auflage, 4. Korrigierter Nachdruck. 2012.

[14] Max Rubner-Institut. Nationale Verzehrsstudie 2. Bundesministerium für Ernährung, Landwirtschaft und Verbraucherschutz. Germany. 2008.

[15] Linseisen J, Bechthold A, Bischoff-Ferrari H. A, Hintzpeter B, Leschik-Bonnet E, Reichrath J, Stehle P, Volkert D, Wolfram G, Zittermann A. Vitamin D Prävention ausgewählter chronischer Krankheiten. DGE. Germany. 2011.

supplementation is required however, seasonal variations have to be considered[16].

A hypervitaminosis D caused by dietary food intake and sun exposure is not known, nevertheless since vitamin D supplementation has become popular over time amongst the general population the toxicity of a high intake should be taken into account[54,55]. Excessive vitamin D consumption causes hypercalcemia, dehydration and tissue calcification[56].

The no observed adverse effect level (NOAEL) for vitamin D is 250 μg/d even though higher dosages show no negative effect but the evidence of those studies and investigations is not strong enough to introduce a NOAEL[55]. The European Food Safety Authority (EFSA) established a tolerable upper intake level (UL) for vitamin D of 100 μg/d with an uncertainty factor of 2.5[17].

The recommended amount of vitamin D intake varies from 600 to 5,000 IU per day for adults between different organizations and is lower for infants and children (see Table 1) (www.vitamindcouncil.org).

	DACH/DGE/ ÖGE	Endocrine Society	Food and Nutrition Board	Vitamin D Council
Infants	400 IU/day	400-1,000 IU/d	400 IU/day	1,000 IU/d
Children	800 IU/day	600-1,000 IU/day	600 IU/day	1,000 IU/day
Adults	800 IU/day	1,500-2,000 IU/day	600 IU/day	5,000 IU/day

Table 1: Recommended daily intake from various organizations (www.vitamindcouncil.org)[18]

[16] Max Rubner-Institut. Nationale Verzehrsstudie 2. Bundesministerium für Ernährung, Landwirtschaft und Verbraucherschutz. Germany. 2008.
[17] EFSA Panel on Dietetic Products, Nutrition and Allergie. Scientific Optinion on the Tolerable Upper Level of Vitamin D. EFSA Journal. Italy. 2012.
[18] Deutsche Gesellschaft für Ernährung, Österreichische Gesellschaft für Ernährung, Schweizerische Gesellschaft für Ernährungsforschung, Schweizerische Vereinigung für Ernährung. Referenzwerte für die Nährstoffzufuhr Vitamin D. Neuer Umschau Buchverlag. 1. Auflage, 4. Korrigierter Nachdruck. 2012.

On account of this the declaration of an appropriate reference intake as well as UL and NOAEL is not yet completely finished and there is still room for more studies and surveys. Also the variation in the change in serum 25(OH)D_3 levels in response to vitamin D supplementation is quite wide from person to person. Factors like dose, duration, baseline 25(OH)D_3, body mass index (BMI), season and age influence the effect of vitamin D supplementation[57,58].
However, a meta regression summarizes that a higher increase in serum levels of 25(OH)D_3 in adults is found with a dose of >800 IU per day, a duration of at least 6-12 months, a lower baseline level and in the oldest elderly[19].

To reach adequate levels of vitamin D, especially in winter, supplementation can be the solution and could provide a safe, low cost therapy with advantages to general, bone and mental health[59,60].

II.XV VDR target genes

Microarray analyses in different tissues and cells and treated on various time points suggest a long list of VDR target genes. However, the overlap between these genes in diverse arrays is rather small and confirms the overall impression that most VDR target genes respond to its ligand in a very tissue- and time-specific way. Nevertheless the majority of these genes show functions in the immune system[32,49-51]. For VDR target gene identification short incubations from two to four hours with 1,25(OH)$_2D_3$ are needed, whereas for overall physiological effects longer treatment times (24 h and more) are essential[61]. The latter contain mostly secondary or tertiary 1,25(OH)$_2D_3$ target genes[53].

The described target genes below were identified in THP-1 cells, 40 min ligand stimulation for VDR location mapping respectively 4 h treatment with 1,25(OH)$_2D_3$ for mRNA expression changes. Due to the short stimulation time these genes can be assumed to be primary vitamin D targets[50].

[19] Shab-Bidar S, Bours S, Geusens P. P. M. M, Kessels A. G. H, van den Bergh J. P. W. Serum 25(OH)D response to vitamin D_3 supplementation: A meta-regression analysis. Nutrition. 2014.

II.XV.I CD97

CD97 encodes a seven-span transmembrane receptor (TM7). The gene is located on the short arm of human chromosome 19[62]. Immune and smooth muscle cells express CD97 as well as monocytes, macrophages, dendritic cells and granulocytes[62]. During lymphocyte activation *CD97* is rapidly up-regulated and led to the definition as an activation marker[62]. Human CD97 exists in three isoforms, with three, four and five epidermal growth factor (EGF) domains[63]. For CD97 two ligands have been identified: CD55/decay accelerating factor (DAF) and chondroitin sulfate. Via its EGF domain region, CD97 is able to bind CD55/DAF. This molecule protects host cells from complement-mediated damage by down-regulation of complement activity. CD55 is expressed at a low level by most epithelial and endothelial cells. Inflammatory signals increase the CD55 expression up to 40-times[3]. It seems that CD55 inhibits complement activity, while docked with CD97, and most probably down-regulates CD97 on circulating leukocytes. This could prevent clustering or inappropriate binding to the endothelium[64]. CD97 engagement of CD55 on naive $CD4^+$ cells incudes IL-10 production by Th1 cells[65]. The affinity for CD55 is higher, the smaller the CD97 isoform and the interaction is Ca^{2+}-dependent[66]. Chondroitin sulfate binds to the biggest isoform of CD97 and appears as component of cell surface proteoglycans and in extracellular matrixes[62,67]. Elevated CD97 expression has been reported in several diseases linked with inflammation[67] and is up regulated in thyroid, but also in colorectal, gastric, esophageal and pancreatic carcinomas[62,68].

II.XV.II LRRC8A

LRRC8A encodes a leucin-rich repeat-containing 8 protein. The gene is located on the long arm of chromosome 9. The LRR's (leucine-rich repeats) are located on the outside of the cell[69]. LRRC8A is expressed in heart, brain, placenta, lung, liver, kidney and pancreas, but not in skeletal muscle cells[69]. Peripheral resting monocytes express LRRC8A, however after macrophages differentiation with lipopolysaccharide stimulation *in vitro*, the LRRC8A mRNA expression is

repressed[69]. Probably, LRRC8A has a specific ligand that induces B cell development. LRRC8A also lacks domains that can transduce signals to the cytosol or nucleus, therefore LRRC8A might have adapter molecules for signal transduction as shown in a TLR on B cells[70]. A lack of LRRC8A is responsible for the B cell deficiency in gammaglobulinemia and for that reason normal LRRC8A expression is required for B cell development, for growth and/or differentiation in pro-B and pre-B cells[70]. LRRC8A is expressed widely beyond lymphoid and hematopoietic system and consequently the protein might play a role in morphogenesis[70]. A potential role of the membrane protein LRRC8A is suggested in the regulation and organization of intracellular signaling cascades as well as the direct or indirect cell-cell communication[71].

II.XV.IIISLC37A2

SLC37A2 encodes a glucose-6-phosphate transporter. The gene is located on the long arm of the human chromosome 11. SLC37A2 is associated with the endoplasmic reticulum membrane and the N-terminus is on the cytoplasmic side of the membrane[72,73]. SLC37A2 is expressed in liver, kidney, intestine and pancreas tissue as well as macrophages, spleen and thymus[72]. *SLC37A2* transcription is increased upon macrophage differentiation in human THP-1 cells and thus seems to play a transport role in macrophage metabolism[74]. Defect in *SLC37A4*, a well-studied member of the SLC37 family, lead to glycogen storage disease type 1b. Patients who suffer from this disease show disrupted glucose homeostasis and immune system complications. It is likely that similar to SLC37A4, SLC37A2 is a key to aspects of immune function, especially with the focus on macrophages[74]. *SLC37A2* is up-regulated in white adipose tissue from obese, compared with wild type tissue in mice. This most likely is the case, because macrophage infiltration in obese white adipose tissue is elevated. It also seems that SLC37A2 acts as a sugar transporter particularly required for macrophages that are present in obese white adipose tissue[74]. The grouping into the SLC37 family, which has four members, is based on sequence homology to bacterial organo-phosphate:Pi exchangers. Therefore it is likely

that the role of the SLC37A2 protein lies in cells outside the gluconeogenic tissue and their biological role is not only linked with the blood glucose homeostasis[72].

II.XV.IV NRIP1

NRIP1 encodes nuclear receptor-interacting protein 1. The gene is located on the long arm of the human chromosome 21[75]. NRIP1 is predominantly located in the nucleus[76]. NRIP1 is widely expressed in metabolic tissue including mature adipocytes[77]. NRIP1 primarily acts as a co-repressor for several nuclear receptors and transcription factors, which are crucial regulators of metabolism, but also co-activator functions are known[75]. These are described in monocytes and macrophages and result in an enhancement of innate inflammation[76]. Co-regulators in general help nuclear receptors to positively or negatively influence the transcription of target genes. The relative level of NRIP1 expression in comparison with other cofactors determines this ability[76]. NRIP1 primarily acts as a scaffold protein that links nuclear receptors to chromatin remodeling enzymes involved in chromatin condensation and thus transcriptional repression[76]. NRIP1 plays a role in regulating inflammatory processes by activating expression of the proinflammatory cytokines IL-6, TNFα and IL1β in macrophages. NRIP1 promotes the ability of cells to develop endotoxin tolerance[75].

II.XV.V THBD

THBD encodes an endothelial-specific type I membrane receptor that binds thrombin. The gene is located on the short arm of the human chromosome 20. THBD is dominantly expressed on endothelial cells of arteries, veins and capillaries and a small amount of soluble THBD (sTHBD) circulates in plasma[78,79]. THBD raises the thrombin-catalyzed activation rate of protein C, which acts as an anticoagulant and has anti-inflammatory effects[78,80]. THBD itself has also an anti-inflammatory effect by binding to the pro-inflammatory thrombin[78]. An epidemiological study indicates an association between a high

level of plasma THBD and a low future risk of coronary heart disease[79]. Furthermore sTHBD suppresses apoptosis in endothelial cells and thus plays a role in endothelial protection[78]. THBD is used in the clinical practice as a treatment for patients with disseminated intravascular coagulation based upon hematologic malignancy[81]. A role for THBD in tumor biology is also suggested, confirmed by the negative correlation between THBD expression and cell proliferation in vitro and in vivo of three different tumor cell lines. This effect seems to be independent of thrombin and the thrombin receptor[82].

II.XV.VI CD14

CD14 encodes a glycosylphosphatidylinositol anchored protein and a soluble serum protein. The gene is located on the long arm of the human chromosome 5[83]. The CD14 protein is located in the endoplasmatic reticulum on the cell surface. CD14 is predominantly expressed in monocytes, macrophages and neutrophils, and at lower levels in epithelial cells, endothelial cells and fibroblasts. Soluble CD14 (sCD14) seems to be a result of cleavage from the surface of monocytes and is present in the circulation and other fluids. Plasma sCD14 levels are increased during inflammation and infection. CD14 acts as a recognition receptor for a variety of microbial ligands and as a receptor for endogenous molecules on the surface of apoptotic cells, amyloid peptides, ceramide and urate crystals[84]. CD14 forms a LPS receptor complex with the transmembrane TLR2 and thus leads to induced expression of cytokines, cell adhesion molecules and low proinflammatory molecules[85,86]. Taken together, CD14 has an impact of several inflammatory diseases, supported by the fact that oxidized LDL binds to CD14, in association with TLR4, and promotes cytokine expression. The competition between LPS and oxidized LDL for the same receptor seems to be regulatory factor in inflammatory situations[87].

II.XV.VII SP100

SP100 encodes a subnuclear organelle and major component of the promyelocytic leukemia (PML)-SP100 nuclear body. The gene is located on the long arm of the human chromosome 2. The localization and protein level of SP100 is modulated by multiple factors like cell cycle, environmental stress or viral infection. For instance the protein localizes to nuclear particles during interphase but disbands from them during mitosis[88]. Nuclear bodies are involved in the pathogenesis of human diseases like acute promyelocytic leukemia and viral infections[89]. SP100 shows diverse cell functions including apoptosis, transcriptional regulation and protection against viral infection[88,90]. SP100 has four alternatively spliced isoforms, SP100 A, B, C and HMG. The last three show domains which suggest the interaction with DNA and chromatin and have a repressive function, in contrast to SP100 A, which promotes transcription[90,91]. SP100 does not bind to DNA alone but seems to interact with DNA via association with specific DNA-binding proteins like heterochromatin protein 1, the B-cell-specific transactivator Bright or the transcription factor ETS1. The latter stimulates expression, in contrast to the other two, which mediate transcriptional repression[89,90].

III Material and Methods

III.I Cell culture

The human acute monocytic leukemia cell line THP-1 was derived from the peripheral blood of a boy with acute monocytic leukemia[92]. The cells grow in suspensions and differentiate into macrophage-like cells using phorbol 12-myristate 13-acetate (PMA)[92]. After differentiation the cells become adherent and change their shape (see Figure 9).

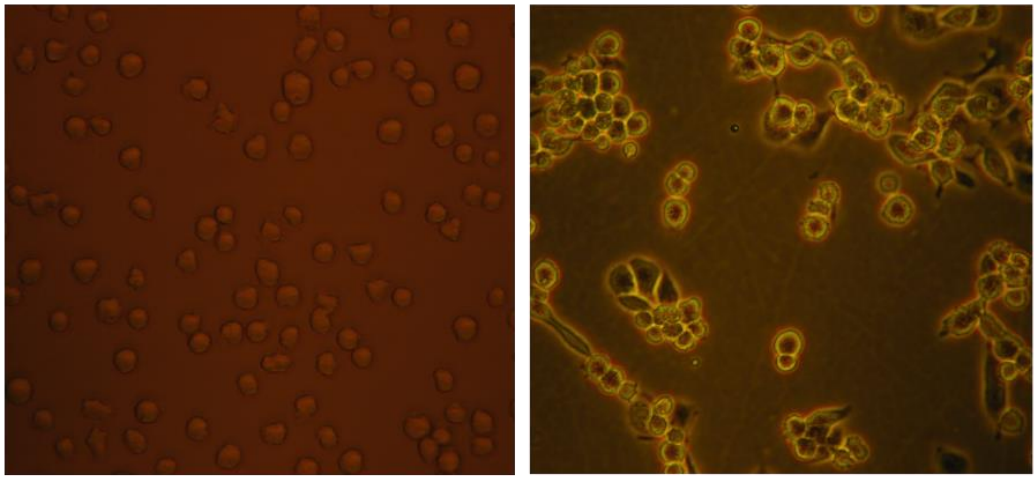

Figure 9: Morphology of undifferentiated and PMA differentiated THP-1 cells. THP-1 cells (left) develop characteristic macrophage morphology after 72 h exposure to PMA (right).

THP-1 cells were grown in RPMI 1640 medium supplemented with 10% fetal calf serum, 2 mM L-glutamine, 0.1 mg/ml streptomycin and 100 U/ml penicillin and the cells were kept at 37 °C in a humidified 95% air / 5% CO_2 incubator. Prior to chromatin or mRNA extraction, undifferentiated THP-1 cells were grown overnight in a density of 0.5 or $0.8x10^6$ cells/ml, respectively, in phenol red-free RPMI 1640 medium supplemented with 5% charcoal-stripped fetal calf serum. The latter has been depleted by non-polar molecules, such as virus, growth factors, hormones and cytokines. Thus, this serum is more defined and lipid-like components, like nuclear receptor ligands, do not influence the research results

(see www.lifetechnologies.com/at/en/home/life-science/cell-culture/mammalian-cell-culture/fbs/specialty-serum/charcoal-stripped-fbs.html).

Two different types of macrophages are known. Macrophage 1 (M1) and macrophage 2 (M2) activities have several functions. M1-type macrophages inhibit cell proliferation and cause tissue damage. M2-type macrophages on the other hand promote cell proliferation and tissue repair. M1 macrophages promote T helper 1 responses and M2 macrophages T helper 2 responses[93]. For differentiation into M2-type macrophage-like cells, THP-1 cells were grown for 72 h in full growth medium supplemented with 20 nM PMA (Sigma-Aldrich) in a density of $0.8x10^6$ cells/1.5 ml for mRNA extraction and 10^7 cells/25 ml for chromatin extraction. Then, the cells were treated with solvent (0.1% ethanol) or 100 nM $1,25(OH)_2D_3$ (Sigma-Aldrich) for the indicated time periods.

III.II RNA extraction, cDNA synthesis and qPCR

Total RNA from undifferentiated and PMA-differentiated THP-1 cells was extracted using the Quick RNA Miniprep Kit (Zymo Research). To isolate RNA different methods are available. In this study anion-exchange silicate-based columns were used. The first step is the homogenization of the tissue and breaking down cells and cell components by adding lysis buffer. Then the sample is transferred to the columns where nucleic acids bind. The separation of DNA and RNA is caused by the different salt concentration of the wash buffers. The last step is the elution of RNA with ribonuclease (RNase) free water.

Complementary deoxyribonucleic acid (cDNA) synthesis was performed with the Transcriptor First Strand cDNA Synthesis Kit (Roche) according to the manufacturer's instructions. The principle of cDNA synthesis is a generation of cDNA from mRNA. Reverse transcriptase acts on a single strand of mRNA and produces its complementary DNA based on the pairing of RNA base pairs. Therefore a primer with a free 3'-hydroxyl group and deoxynucleotide triphosphates (dNTPs) are needed (see www.roche-applied-science.com). 1 µg

of total RNA was used as a template and the synthesis was carried out at 55 °C for 30 min. Prior to qPCR the cDNA was diluted 20-fold.

qPCR is used for the quantification of nucleic acid sequences and seems to be a gold standard for gene expression analysis. Primers are designed to specifically bind the target DNA added to the reaction. The action of the Taq polymerase extends the primers during repeated cycles of heat-denaturation, primer annealing and primer extension. Each cycle leads to a doubling of the DNA and for that reason the reaction proceeds in an exponential manner. After a number of cycles one of the reagents becomes limiting and the reaction reaches a plateau[20].

As detection methods different fluorescent technologies are applicable and in this study SYBRGreen, a dye for non-specific detection, was used. SYBRGreen intercalates into a double-stranded DNA and emits light of 520 nm wavelength once bound there. The amount of bound SYBRGreen is proportional to the amount of generated target[20].

At the end of the qPCR run it is recommended to run a melt curve analysis. Therefor, the temperature is slowly increased and at a certain point, depending on length and composition of the amplicon, the whole amplified product will fully dissociate. The result is a drop of fluorescence as the SYBRGreen dissociates from the double-stranded DNA and thus it is possible to check how many products are present in the well. If there is more than one dissociation peak the amplification is not specific because more than one product has been generated[20].

qPCR reactions were performed using 250 nM of reverse and forward primers (see Table 2), 2 µl 1/20 diluted cDNA template and the LightCycler 480 SYBRGreen I Master mix (Roche) in a total volume of 10 µl. In the PCR reaction the hotstart Taq polymerase was activated for 10 min at 95 °C, followed by 40 amplification cycles of 20 s denaturation at 95 °C, 15 s annealing at primer-specific temperatures (see Table 2) and 15 s elongation at 72 °C and

[20] Vandesompele J. qPCR guide. Eurogentec Experience true partnership. Downloaded at www.eurogentec.com/uploads/qPCR-guide.pdf January 2014.

a final elongation for 10 min at 72 °C. PCR product specificity was monitored using post-PCR melt curve analysis. Relative expression levels were determined with the comparative delta threshold cycle (ΔCt) method. This method is used for quantifying the relative changes in gene expression and compares Ct values between the target gene and the reference genes. The Ct value is a number of cycles at which the amount of amplified target reaches a fixed threshold. Thus this value is inverse proportional to the expression level of the gene. If the Ct value is low, the amount of target in the sample is high [94,21]. Relative expression levels of the target genes were normalized to the three internal reference genes beta-2-microglobulin *(B2M)*, gylcerinaldehyde-3-phosphate-dehydrogenase *(GAPDH)* and hypoxanthine phosphoribosyltransferase 1 *(HPRT1)*. The stability of the expression of the reference genes was determined using the geNorm algorithm[95]. Briefly, the arithmetic mean of replicated Ct values for each gene is transformed to a relative quantity (setting the sample with the highest expression as calibrator to 1), using the ΔCt formula $Q = 2^{\Delta Ct} = 2^{(calibratorCt - sampleCt)}$ (Q = quantity sample relative to calibrator sample). For normalization, the relative quantities were divided by the normalization factor being the geometric mean of the three reference genes.

Gene	Fragment size (bp)	Annealing temperature (°C)	Primer sequences (5'-3')
B2M[1,3]	246	60	GGCTATCCAGCGTACTCCAAA
			CGGCAGGCATACTCATCTTTTT
CD14[2]	142	60	ACGCCAGAACCTTGTGAGC
			GCATGGATCTCCACCTCTACTG
CD97[2]	133	60	GGGACAAGAACGTCACTATGG
			GCCAGCAATGTCGTCATGT
GAPDH[1,3]	113	60	CATGAGAAGTATGACAACAGCCTA
			GTCCTTCCACGATACCAAAGT
HPRT1[1,3]	94	60	TGACACTGGCAAAACAATGCA

[21] Vandesompele J. qPCR guide. Eurogentec Experience true partnership. Downloaded at www.eurogentec.com/uploads/qPCR-guide.pdf January 2014.

			GGTCCTTTTCACCAGCAAGCT
LRRC8A[2]	205	60	CCACCCAGCTCTTCTACTGC
			AGTGACTGCAGCACGTTGTT
NRIP1[2]	179	60	TGGAATGCAGTCATCCATGT
			CTGGTTCAGGACCTGTTGGT
SLC37A2[2]	240	60	GGAAGCCTATCAGTATCGTCAAG
			CTGAGAGGTAGTAACGGAGCG
THDB[2]	107	66	GACCTTCCTCAATGCCAGTCA
			CGTCGCCGTTCAGTAGCAA

Table 2: Reverse transcripton qPCR primers

[1] reference gene

[2] sequence obtained from PrimerBank (http://pga.mgh.harvard.edu/primerbank)

[3] see [95]

III.III Samples of the VitDmet study

The participants of the VitDmet study (NCT01479933, ClinicalTrials.gov) were selected to be ≥60 years of age for males or ≥65 for females, showed evidence of disturbed glucose homeostasis, impaired fasting glucose or impaired glucose tolerance, but no type 2 diabetes, and had a BMI between 25 and 35. From 73 individuals we selected 71, for which PBMC isolates were available from both the start and the end of the trial. The research ethics committee of the Northern Savo Hospital District had approved the study protocol. All participants gave a written informed consent to participate in the study (for further details see[96]).

Serum 25(OH)D_3 concentrations were measured from venous blood samples using a high performance liquid chromatography with coulometric electrode array as described previously[97]. The baseline serum 25(OH)D_3 concentrations ranged between 35.9 and 73.6 nM at the start of the intervention and raised in average by 24.9 nM. The measurement of other basic clinical and biochemical variables showed that neither the BMI nor serum calcium concentrations significantly changed during the intervention. The participants took a vitamin D_3

supplement with 0, 40 or 80 μg daily over 5 month. (for further details see[22,96]). PBMCs were isolated from 8 ml of peripheral blood in a Vacutainer CPT Cell Preparation Tube with sodium citrate (BD)[98]. Total RNA was extracted using the TRIzol method followed by further purification with miRNeasy Mini Kit columns (Qiagen) and reverse transcribed into cDNA using the High-Capacity cDNA Archive Kit (Applied Biosystems). qPCR was performed as described above.

III.IV ChIP-qPCR

After treatment of undifferentiated and PMA-differentiated THP-1 cells, nuclear proteins were cross-linked to DNA by adding formaldehyde directly to the medium to a final concentration of 1% and incubating at room temperature for 5 min on a rocking platform. Cross-linking was stopped by adding glycine to a final concentration of 0.125 M and incubating at room temperature for 5 min on a rocking platform. The cells were collected by centrifugation and washed twice with ice-cold phosphate buffered saline (PBS). The cell pellets were resuspended in 1900 µl of lysis buffer (1% SDS, 10 mM EDTA, protease inhibitors, 50 mM Tris-HCl, pH 8.1) and the lysates were sonicated in a Bioruptor Plus (Diagenode) to result in DNA fragments of 200 to 400 bp. The sonication was performed in 15 ml Bioruptor tubes for 40 or 45 min, with 30 s ON, 30 s OFF cycles. After each 10 min the tubes were shaked. Cellular debris was removed by centrifugation. 200 µl aliquots of the lysate were diluted 1:9 in ChIP dilution buffer (0.01% SDS, 1.1% Triton X-100, 1.2 mM EDTA, 167 mM NaCl, protease inhibitors, 250 µg/ml BSA, 16.7 mM Tris-HCl, pH 8.1). 1 µg of anti-VDR antibody (sc-1008X, Santa Cruz Biotechnology) or non-specific IgG (12-370, Millipore) were bound to 20 µl Magna ChIP Protein A Magnetic Beads (Millipore) in an 3 h to overnight incubation at 4 °C. The pre-formed bead-antibody complexes were then washed three times with ChIP dilution buffer and added to the chromatin aliquots (1 µg antibody and 20 µl beads per output aliquot). The samples were incubated overnight at 4 °C on a rotating platform to

[22] Tuomainen TP, Voutilainen S, Virtanen J, Nurmi T, Mursu J, et al. (2013) Glucose metabolism effects of vitamin D supplementation in prediabetes – the VitDmet study. submitted.

form and collect the immuno-complexes. The beads were washed sequentially for 3 min on a rotating wheel with 1 ml of the following buffers: low salt wash buffer (0.1% SDS, 1% Triton X-100, 2 mM EDTA, 150 mM NaCl, 20 mM Tris-HCl, pH 8.1), high salt wash buffer (0.1% SDS, 1% Triton X-100, 2 mM EDTA, 500 mM NaCl, 20 mM Tris-HCl, pH 8.1) and LiCl wash buffer (0.25 M LiCl, 1% Nonidet P-40, 1% sodium deoxycholate, 1 mM EDTA, 10 mM Tris-HCl, pH 8.1). Finally, the beads were washed twice with 1 ml TE buffer (1 mM EDTA, 10 mM Tris-HCl, pH 8.0) and the immune complexes were eluted twice with 250 µl elution buffer (1% SDS, 100 mM NaHCO3) at room temperature for 15 min with rotation. The supernatants were combined and the immune complexes were reverse cross-linked at 65 °C from 4 h to overnight in the presence of proteinase K (Roche) in a final concentration of 40 µg/ml. The DNA was isolated with the ChIP DNA Clean&Concentrator Kit (Zymo Research). The ChIP DNA Binding Buffer in this Kit promotes DNA adsorption to the matrix of the column in the presence of antibodies, detergents and proteinases. After two wash steps the DNA is ready for elution with a small volume of water[23].

DNA concentrations were determined with the Quant-iT dsDNA HS assay (Invitrogen). This Kit uses the fluorophore Picogreen, which becomes fluorescent upon binding to DNA, RNA or protein. The Quanti-iT ds DNA HS assay selects double-stranded DNA over RNA and in the range of 0,2-100 ng the fluorescence signal is linear to the DNA concentration[24].

To control the DNA fragment sizes, DNA was extracted from 30 µl reverse-crosslinked chromatin with phenol/chloroform/isoamyl alcohol (25/24/1) and precipitated with 0.1 volumes of 3 M sodium acetate, pH 5.2, and 2 volumes of ethanol using glycogen as a carrier. Subsequently, the DNA was resolved on a 1% agarose gel.

Selected genomic regions containing VDR ChIP-seq peaks were analyzed by qPCR using equal DNA amounts of chromatin fragments, LightCycler 480 SYBRGreen I Master mix (Roche) and the specific primer pairs (see Table 3).

[23] Zymo Research. Instruction manual. ChIP DNA Clean & Concentrator. Catalog Nos. D5201 & D5205. Downloaded at www.zymoresearch.com/downloads/dl/file/id/78/d5201i.pdf January 2014.

[24] Nucleic Acid and Protein Quantitation. The Qubit Quantitation Platform. Downloaded at www.mobitec.com/download/flyer/Qubit_web.pdf January 2014.

The qPCR reactions were performed using the following profile: 10 min at 95 °C, followed by 45 cycles of 20 s at 95 °C, 15 s at primer-specific annealing temperature (see Table 3) and 15 s at 72 °C and a final amplification step of 10 min at 72 °C. The results were normalized with respect to input using the formula $2^{-(\Delta Ct)}$x100, where ΔCt is $Ct_{(input)} - Ct_{(immunoprecipitated\ DNA)}$ and Ct is the fractional cycle number.

Genomic region	Fragment size (bp)	Annealing temperature (°C)	Primer sequences (5'-3')
CD97[1]	114	60	TAAGGCCTCACCCTGATGAC
			TGTGCCCCTCCAAATTAAAA
LRRC8A[1]	159	60	GGATACCCAGCAAACTGAGC
			AAAAAGGCAACAATCGCAAC
MB exon 2[2]	76	60	AAGTTTGACAAGTTCAAGCACCTG
			TGGCACCATGCTTCTTTAAGTC
NRIP1 P1[1]	116	60	TCAGGAAGGTCACAGGGGTC
			TGAGTGGGAGCTACAGCTGA
NRIP1 P2[1]	112	60	GTGGGAAACGCCAGTTACAC
			TGCTGACCCTGGCTACATTA
SLC37A2[1]	126	65	CTCTTCCACCCTGCTGTTTC
			TCGAAACCTTGCTGCTACCT
SP100[1]	95	60	AGCTGACCGGGACACTCTAA
			GAGGAAGGCTGAGGGGTGAA

Table 3: ChIP-qPCR primers.

[1] designed using Primer3Plus (www.bioinformatics.nl/primer3plus)

[2] negative control (Red ChIP Kit (Diagenode))

III.V FAIRE-qPCR

FAIRE analysis was conducted according to the protocol published by Giresi et al[33]. Briefly, THP-1 cells were cross-linked identically as for ChIP. After 5 min cross-linking with formaldehyde (final concentration of 1%) and stopping with glycine (final concentration of 0.125 M) the washed cell pellets were resuspended and incubated sequentially in 2 ml of buffer L1 (50 mM HEPES-KOH, pH 7.5, 140 mM NaCl, 1 mM EDTA, 10% glycerol, 0.5% NP-40, 0.25% Triton X-100), 2 ml of buffer L2 (10 mM Tris-HCl, pH 8.0, 200 mM NaCl, 1 mM EDTA, 0.5 mM EGTA) and 700 µl of buffer L3 (10 mM Tris-HCl, pH 8.0, 100 mM NaCl, 1 mM EDTA, 0.5 mM EGTA, 0.1% Na-Deoxycholate, 0.5% N-lauroylsarcosine). The lysates were sonicated in the Bioruptor Plus (Diagenode) to result in DNA fragments of 300 to 500 bp. Cellular debris was removed by centrifugation and input samples were reverse cross-linked overnight at 65 °C. The reverse cross-linked reference samples and the FAIRE samples were subjected to two sequential phenol/chloroform extractions in Phase Lock Gel Heavy tubes (5 Prime), resuspended in 10 mM Tris-HCl (pH 7.4) and treated with 1 µl of RNase A (10 mg/ml) for 1 hour at 37 °C. The DNA was purified with the ChIP DNA Clean & Concentrator Kit (Zymo Research) (for details see chapter ChIP-seq above). For DNA sequencing the Solexa Gene Analyzer 2 platform at the Genomics Core Facility at the EMBL was used. Statistically significant peaks were identified using the Zinba program package version 1.06 by setting the mean fragment length at 200 bp and using other settings as recommended for FAIRE-seq in the Zinba website (http://code.google.com/p/zinba/winki/UsingZINBA) including peak refinement.

For FAIRE-qPCR chromatin templates were prepared in the same way as for FAIRE-seq. qPCR was performed using the same primer pairs and conditions as described for ChIP-qPCR. In short, the selected peaks were analyzed by qPCR using equal DNA amounts of chromatin fragments, 250 nM of reverse and forward primers and Light Cycler 480 SYBRGreen I master mix. The PCR reactions were performed using the following profile: 10 min at 95 °C, followed by 45 cycles of 20 s at 95 °C, 15 s at primer-specific temperatures and 15 s at 72 °C and a final amplification step of 10 min at 72 °C.

III.VI ChIP-seq, FAIRE-seq and ChIA-PET data visualization

The VDR ChIP-seq (GSE27437) and FAIRE-seq (GSE40075) datasets of undifferentiated THP-1 cells are available at GEO (www.ncbi.nlm.nih.gov/geo). The Integrative Genomics Viewer (IGV)[99] was used to visualize ChIP-seq and FAIRE-seq data. The ChIA-PET data for CTCF-mediated chromatin loops in K562 human monocytic leukemia cells (wgEncodeEH002075) was visualized using the UCSC genome browser (http://genome.ucsc.edu)[100].

III.VII Data analysis

Linear regression analysis was performed using Microsoft Excel, version 2011. The ranking of vitamin D responsiveness was done under the assumption of a linear positive correlation between changes of the mRNA expression of the VDR target genes and alterations in the serum 25(OH)D_3 concentrations. The study participants were sorted according to their ratios of gene expression and serum 25(OH)D_3 concentration changes in ascending order (for each gene separately). Starting from the mean all individuals were then ranked symmetrically for each VDR target gene.

IV Results

IV.I VDR binding sites close to 1,25(OH)$_2$D$_3$ target genes

Based on our genome-wide screening for VDR binding sites and transcriptome-wide analysis of primary 1,25(OH)$_2$D$_3$ target genes in undifferentiated THP-1 cells[50], we selected the genes *CD97*, *LRRC8A*, *SLC37A2* and *NRIP1* for more detailed investigations. VDR ChIP-seq data suggest that the *CD97* gene has a prominent VDR binding site (P1$_{CD97}$) 56 kb upstream and a minor VDR binding site (P2$_{CD97}$) 250 kb upstream of its TSS (see Figure 10A). Both sites are active in undifferentiated THP-1 cells (red tracks) but not in PMA-differentiated THP-1 cells (green tracks). A dominant VDR site (P1$_{LRRC8A}$) 0.8 kb downstream and a minor VDR site (P2$_{LRRC8A}$) 140 kb upstream of the *LRRC8A* TSS are both receptor occupied in undifferentiated THP-1 cells. However VDR binding to the major site (P1$_{LRRC8A}$) occurs already in the absence of ligand while at the minor site (P2$_{LRRC8A}$) VDR binding disappears after ligand treatment. In PMA-differentiated THP-1 cells VDR binds only to P1$_{LRRC8A}$ (see Figure 10B). The *SLC37A2* gene has only one site (P$_{SLC37A2}$) located 7.5 kb downstream of its TSS, which is bound by VDR both in undifferentiated and PMA-differentiated THP-1 cells (see Figure 10C). In both cellular models a stronger site (P1$_{NRIP1}$) 158 kb upstream of the *NRIP1* TSS and a weaker site (P2$_{NRIP1}$) 143 kb upstream are associated with VDR (see Figure 10D).

We displayed the genomic loci of the four genes in a scale that provides an overview on the chromatin domains at the respective sites. For this purpose we used ChIA-PET data for the transcription factor CTCF, which were obtained in K562 cells[101] (dark blue in Figure 10) that are rather similar to THP-1 cells[102]. CTCF binding sites are highly conserved between cell types and are assumed to define the borders of chromatin domains[103]. Therefore, it is very likely that the same chromatin loops are also formed in THP-1 cells[36]. The sizes of the core chromatin domains of the genes *CD97*, *LRRC8A*, *SLC37A2* and *NRIP1* (red horizontal lines in Figure 10) are 7.3, 64, 129 and 956 kb, respectively, and

were determined by the distance between the closest strong ChIA-PET CTCF peaks left and right of the major VDR binding sites. Since the core chromatin domain around $P1_{CD97}$ does not contain the TSS of the *CD97* gene (see Figure 10A), we assume that in this case some of the larger chromatin loops, as indicated by ChIA-PET data, are used for the VDR-dependent regulation of the gene. Also, for the *SLC37A2* locus the ChIA-PET looping data indicate the formation of two slightly bigger loops rather than the minimal core loop, while for the *NRIP1* region no loops were detected in K562 cells.

In summary, the core chromatin domains of the genes *CD97*, *LRRC8A*, *SLC37A2* and *NRIP1* vary significantly in size (7.3 to 956 kb) and contain each one major VDR binding site. In undifferentiated THP-1 cells all these sites are occupied by VDR, while only the sites of *LRRC8A*, *SLC37A2* and *NRIP1* are receptor-bound in PMA-differentiated THP-1 cells.

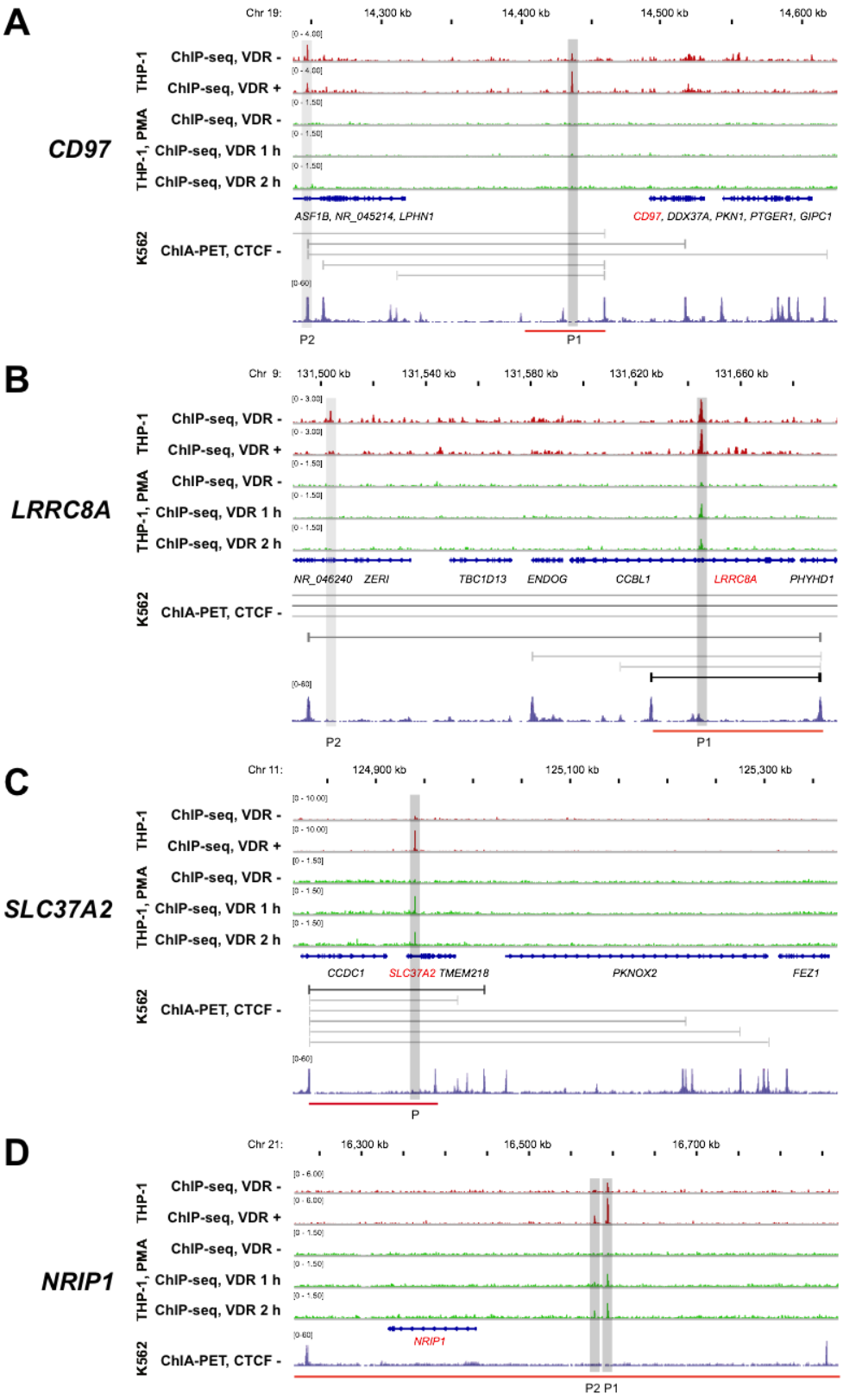
A
CD97
Chr 19:
14,300 kb
14,400 kb
14,500 kb
14,600 kb
THP-1
ChIP-seq, VDR -
ChIP-seq, VDR +
THP-1, PMA
ChIP-seq, VDR -
ChIP-seq, VDR 1 h
ChIP-seq, VDR 2 h
ASF1B, NR_045214, LPHN1
CD97, DDX37A, PKN1, PTGER1, GIPC1
K562
ChIA-PET, CTCF -
P2
P1
B
LRRC8A
Chr 9:
131,500 kb
131,540 kb
131,580 kb
131,620 kb
131,660 kb
NR_046240
ZERI
TBC1D13
ENDOG
CCBL1
LRRC8A
PHYHD1
C
SLC37A2
Chr 11:
124,900 kb
125,100 kb
125,300 kb
CCDC1
SLC37A2
TMEM218
PKNOX2
FEZ1
P
D
NRIP1
Chr 21:
16,300 kb
16,500 kb
16,700 kb
NRIP1
P2 P1

Figure 10: Chromatin domains containing VDR binding sites. The IGV browser was used to display the chromatin domains containing the genes *CD97* (A), *LRRC8A* (B), *SLC37A2* (C) and *NRIP1* (D). VDR ChIP-seq data from undifferentiated THP-1 cells[50] (unstimulated (-) and treated for 40 min with 1,25$(OH)_2D_3$ (+), red) and PMA-differentiated THP-1 cells (unstimulated (-) and treated for 1 and 2 h with 1,25$(OH)_2D_3$, green) are shown along with CTCF ChIA-PET looping (grey horizontal lines) and binding site (dark blue) data from K562 cells[101]. Please note that for *NRIP1* (D) no looping view was available in K562 cells from ENCODE. The core chromatin loops are indicated by horizontal red lines. The area of the genomic regions was adapted to the size of the chromatin loops, but for *NRIP1* (D) it did not cover the whole chromatin domain of 956 kb. Gene structures are shown in blue. Dominant VDR peak regions are highlighted in grey, while less minor regions are shaded in light grey.

IV.II 1,25$(OH)_2D_3$-dependent VDR association

In order to confirm the VDR binding sites of the genes *CD97*, *LRRC8A*, *SLC37A2* and *NRIP1*, which have been identified by ChIP-seq data (Figure 10), we performed ChIP-qPCR with independent chromatin samples obtained both from undifferentiated and PMA-differentiated THP-1 cells (see Figure 11). In undifferentiated cells VDR binding to $P1_{CD97}$ was increased after stimulation with 1,25$(OH)_2D_3$, while in PMA-differentiated cells no significant VDR binding to this site could be observed (see Figure 11A) compared to a negative control region of exon 2 of the myoglobin (*MB*) gene (see Figure 12A). Moreover, VDR binding to $P1_{LRRC8A}$ (see Figure 11B), $P1_{SLC37A2}$ (see Figure 11C) and $P1_{NRIP1}$ (see Figure 11D) could be approved in both cellular models. In addition, $P2_{NRIP1}$ was confirmed in undifferentiated but not in PMA-differentiated THP-1 cells (see Figure 11D). Our ChIP-seq analysis[50] suggested for $P2_{CD97}$ and $P2_{LRRC8A}$ no statistically significant VDR binding loci. For all confirmed sites ($P1_{CD97}$, $P1_{LRRC8A}$, $P_{SLC37A2}$, $P1_{NRIP1}$ and $P2_{NRIP1}$) we observed an 1,25$(OH)_2D_3$-dependent increase of VDR binding but no significant difference between 1 and 2 h ligand treatments. In undifferentiated THP-1 cells, the maximal VDR binding to $P1_{CD97}$, $P1_{LRRC8A}$, $P1_{SLC37A2}$, $P1_{NRIP1}$ and $P2_{NRIP1}$ was 23, 21, 54, 38 and 24% in relation to the strong VDR binding site of the SP100 nuclear antigen (*SP100*, see Figure 12B), while in PMA-differentiated THP-1 cells the maximal VDR binding to $P1_{LRRC8A}$, $P1_{SLC37A2}$ and $P1_{NRIP1}$ were 16, 36 and 59% of the reference.

Taken together, both in undifferentiated and PMA-differentiated THP-1 cells ChIP-qPCR confirmed the VDR binding pattern to the sites of the genes *CD97*, *LRRC8A*, *SLC37A2* and *NRIP1* as observed by ChIP-seq.

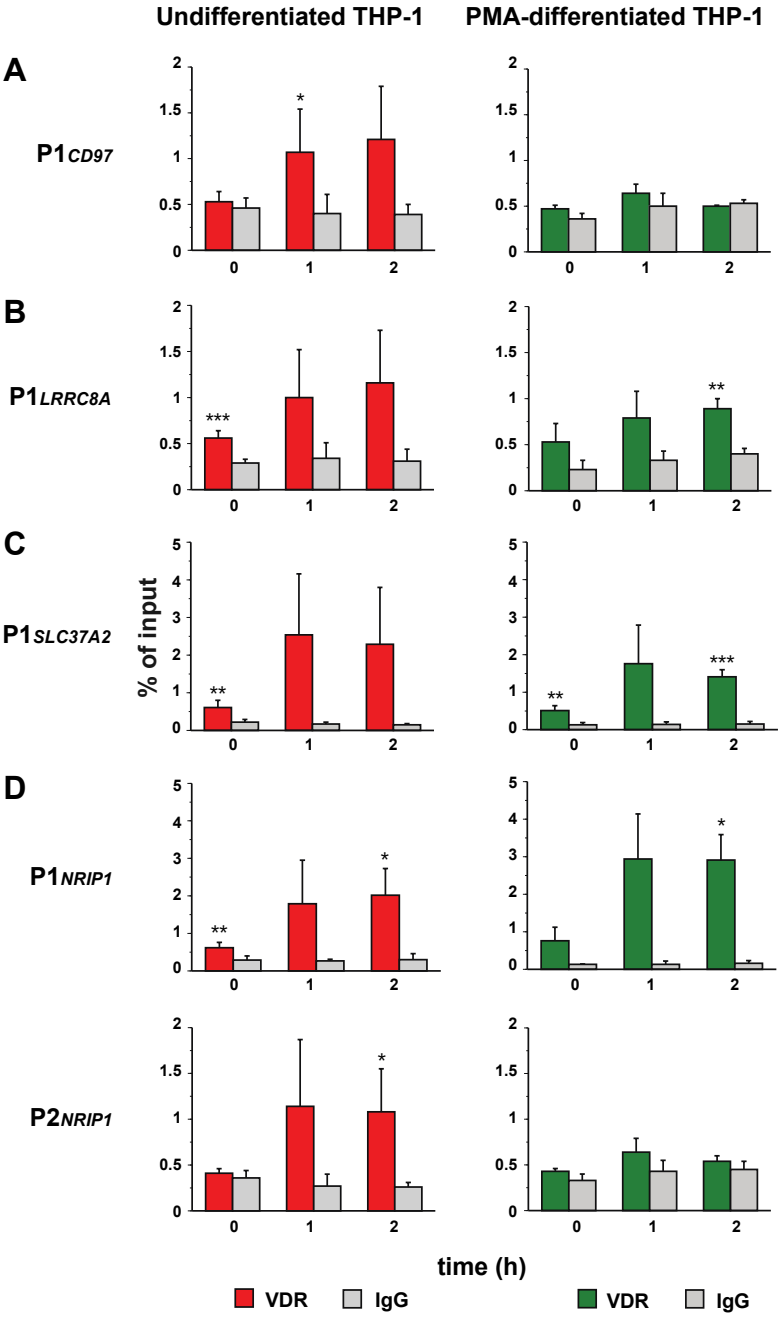

Figure 11: VDR association with genomic regions of target genes. Undifferentiated THP-1 cells (left) and PMA-differentiated THP-1 cells (right) were stimulated for 0, 1 and 2 h with 100 nM $1,25(OH)_2D_3$ and chromatin was extracted. ChIP-qPCR was performed to determine VDR association (red/green) and unspecific IgG binding (grey) at the VDR binding sites of the genes *CD97* (A), *LRRC8A* (B) and *SLC37A2* (C) and at the two sites of *NRIP1* (D). Columns represent the means of at least three independent experiments and the bars indicate standard deviations. Two-tailed Student's t-tests were performed to determine the significance of VDR association in reference to the IgG control (* $p < 0.05$; ** $p < 0.01$; *** $p < 0.001$).

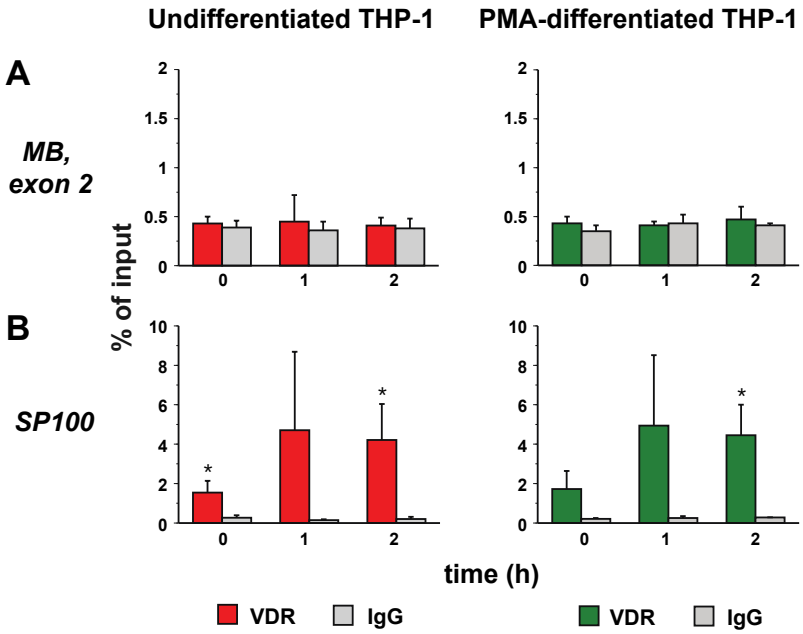

Figure 12: VDR ChIP-qPCR negative and positive control. Undifferentiated THP-1 cells (left) and PMA-differentiated THP-1 cells (right) were stimulated for 0, 1 and 2 h with 100 nM $1,25(OH)_2D_3$ and chromatin was extracted. ChIP-qPCR was performed to determine VDR association (red/green) and unspecific IgG binding (grey) to a negative control region within exon 2 of the *MB* gene (A) and at strong VDR binding site of the *SP100* gene (B). Columns represent the means of at least three independent experiments and the bars indicate standard deviations. Two-tailed Student's t-tests were performed to determine the significance of VDR association in reference to IgG control (* $p < 0.05$; ** $p < 0.01$; *** $p < 0.001$).

IV.III Chromatin accessibility at VDR binding sites

Most efficient VDR binding to its genomic loci requires accessible chromatin in combination with DR3-type binding sequences. Therefore, we used FAIRE-seq data from undifferentiated and PMA-differentiated THP-1 cells for a detailed view on the VDR binding sites of the genes *CD97*, *LRRC8A*, *SLC37A2* and *NRIP1* (Figures 13 and 14). We observed in undifferentiated THP-1 cells at $P1_{CD97}$ clear $1,25(OH)_2D_3$-induced chromatin opening, while in PMA-differentiated THP-1 cells the chromatin was not accessible at this site (see Figure 13A). At $P2_{CD97}$ we could detect accessible chromatin, but $1,25(OH)_2D_3$ had no effect on chromatin opening (see Figure 14A). Neither at $P1_{CD97}$ nor at $P2_{CD97}$ a DR3-type binding sequence was identified. In both cellular models $P1_{LRRC8A}$ is associated with a low $1,25(OH)_2D_3$-inducible FAIRE signal and it also carries a DR3-type sequence below the peak summit (see Figure 13B). In

contrast, $P2_{LRRC8A}$ shows only very weak (in differentiated THP-1 cells) or not detectable (in PMA-differentiated THP-1 cells) signs of open chromatin and does not accommodate any DR3-type sequence (see Figure 14B). $P_{SLC37A2}$ involves a DR3-type sequence and is in differentiated THP-1 cells associated with a strong ligand-inducible FAIRE signal, but in PMA-differentiated cells this VDR binding site shows far weaker signs of open chromatin (see Figure 13C). Both $P1_{NRIP1}$ and $P2_{NRIP1}$ enclose a DR3-type sequence and are located in undifferentiated THP-1 cells within accessible chromatin, which slightly further opens after ligand treatment (see Figure 13D). In contrast, in PMA-differentiated THP-1 cells $P1_{NRIP1}$ is only weakly and $P2_{NRIP1}$ not at all associated with open chromatin and no ligand effect is detectable.

In summary, in undifferentiated THP-1 cells the major VDR binding sites of the genes *CD97*, *LRRC8A*, *SLC37A2* and *NRIP1* are associated with open chromatin, while in PMA-differentiated cells the chromatin is less accessible or, in case of $P1_{CD97}$, even closed. The latter VDR site also does not contain any DR3-type sequence, while the three other major sites do.

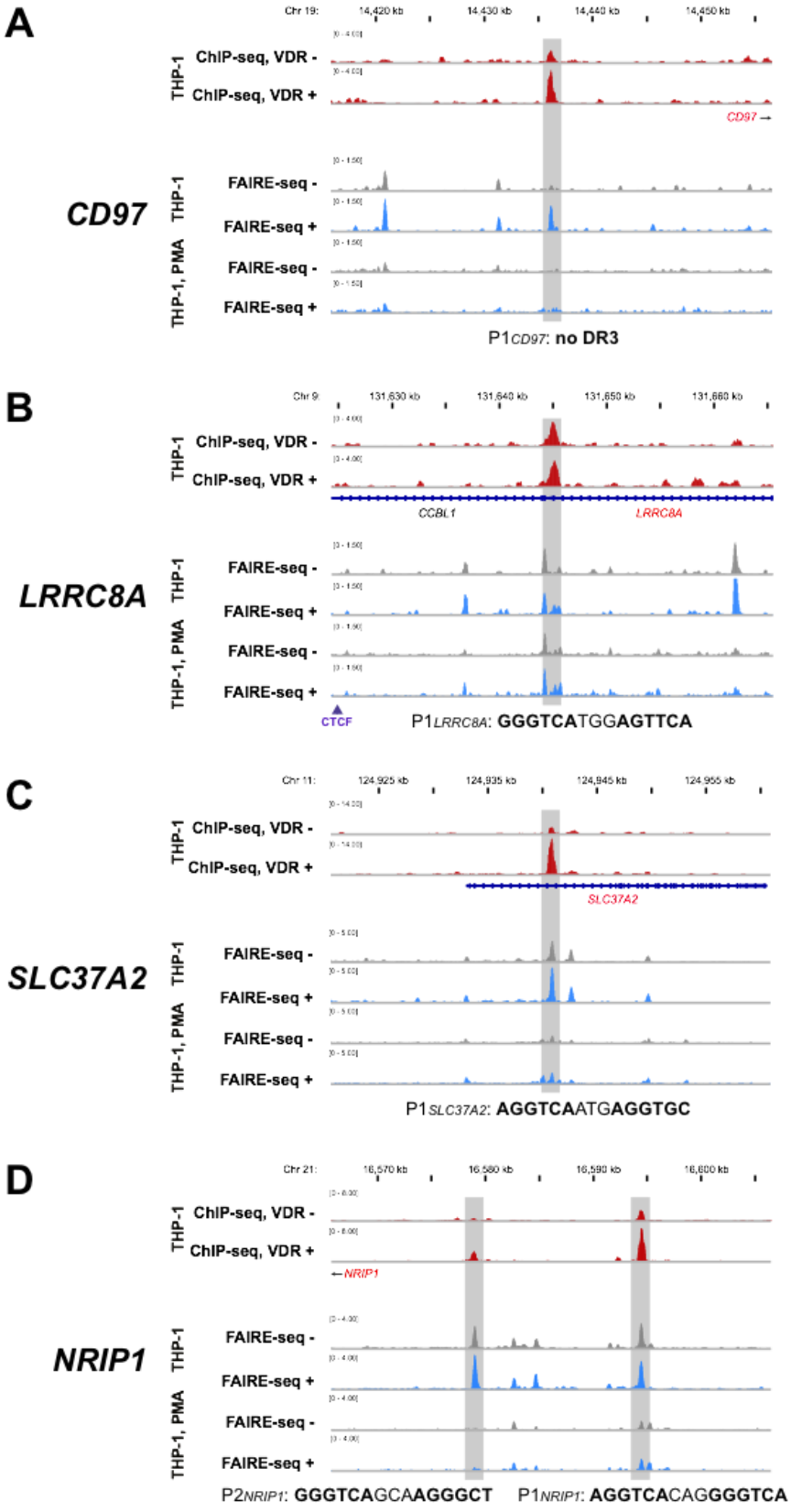
A
Chr 19:
14,420 kb
14,430 kb
14,440 kb
14,450 kb
THP-1
ChIP-seq, VDR -
ChIP-seq, VDR +
CD97
CD97
THP-1
FAIRE-seq -
FAIRE-seq +
THP-1, PMA
FAIRE-seq -
FAIRE-seq +
P1CD97: no DR3
B
Chr 9:
131,630 kb
131,640 kb
131,650 kb
131,660 kb
THP-1
ChIP-seq, VDR -
ChIP-seq, VDR +
CCBL1
LRRC8A
LRRC8A
THP-1
FAIRE-seq -
FAIRE-seq +
THP-1, PMA
FAIRE-seq -
FAIRE-seq +
CTCF
P1LRRC8A: GGGTCATGGAGTTCA
C
Chr 11:
124,925 kb
124,935 kb
124,945 kb
124,955 kb
THP-1
ChIP-seq, VDR -
ChIP-seq, VDR +
SLC37A2
SLC37A2
THP-1
FAIRE-seq -
FAIRE-seq +
THP-1, PMA
FAIRE-seq -
FAIRE-seq +
P1SLC37A2: AGGTCAATGAGGTGC
D
Chr 21:
16,570 kb
16,580 kb
16,590 kb
16,600 kb
THP-1
ChIP-seq, VDR -
ChIP-seq, VDR +
NRIP1
NRIP1
THP-1
FAIRE-seq -
FAIRE-seq +
THP-1, PMA
FAIRE-seq -
FAIRE-seq +
P2NRIP1: GGGTCAGCAAGGGCT
P1NRIP1: AGGTCACAGGGGTCA

Figure 13: Open chromatin in undifferentiated and PMA-differentiated THP-1 cells. The IGV browser was used to visualize the loci of the major VDR binding regions (+/-20 kb of the peak summit) of the genes *CD97* (A), *LRRC8A* (B), *SLC37A2* (C) and *NRIP1* (D). The peak tracks display VDR ChIP-seq data[50] from undifferentiated THP-1 cells (unstimulated (-) and treated for 40 min with 1,25(OH)$_2$D$_3$ (+), red) and FAIRE-seq datasets[61] from undifferentiated and PMA-differentiated THP-1 cells (stimulated for 100 min with EtOH (-, grey) or 1,25(OH)$_2$D$_3$ (+, light blue)). Gene structures are shown in blue, VDR peak regions are shaded in grey and CTCF sites are indicated by violet triangles. In the bottom lines the sequences of DR3-type binding sites within +/-100 bp of the VDR peak summit are indicated.

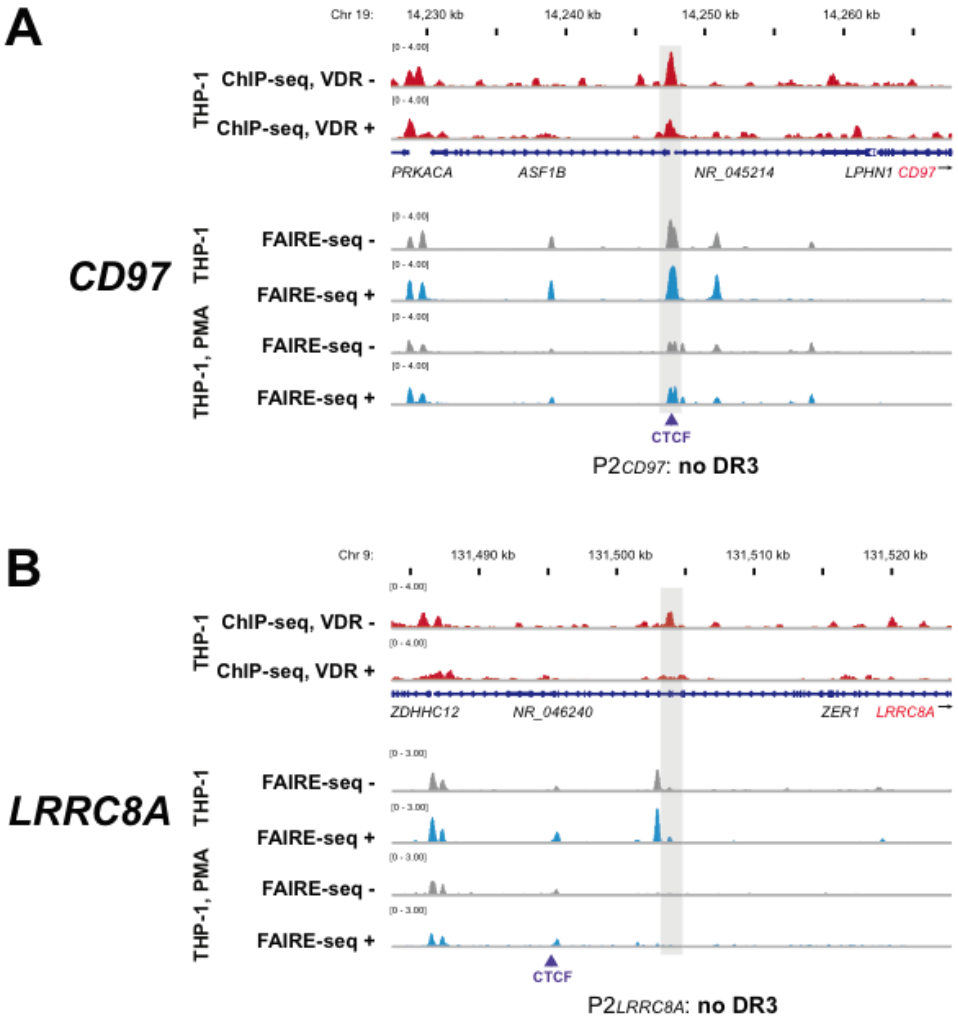

Figure 14: Minor VDR binding sites at the CD97 and LRRC8A loci. The IGV browser was used to visualize the minor VDR binding regions (+/-20 kb of the peak summit) of the genes *CD97* (A) and *LRRC8A* (B). The peak tracks display VDR ChIP-seq data[50] from undifferentiated THP-1 cells (unstimulated (-) and treated for 40 min with 1,25(OH)$_2$D$_3$ (+), red) and FAIRE-seq datasets[61] from undifferentiated and PMA-differentiated THP-1 cells (stimulated for 100 min with EtOH (-, grey) or 1,25(OH)$_2$D$_3$ (+, light blue)). Gene structures are shown in blue, VDR peak regions are shaded in grey and CTCF sites are indicated by violet triangles.

IV.IV 1,25(OH)$_2$D$_3$-dependent mRNA expression

The functional consequences of occupied VDR binding sites, open chromatin and the presence of DR3-type binding sites for the expression of the genes *CD97*, *LRRC8A*, *SLC37A2* and *NRIP1* were tested by performing qPCR in undifferentiated and PMA-differentiated THP-1 cells 2, 4, 6, and 24 h after onset of stimulation with 1,25(OH)$_2$D$_3$ (see Figure 15). In undifferentiated THP-1 cells the mRNA expression of all four genes was statistically significantly up-regulated already after 2 h ligand stimulation and reached a maximal induction after 24 h of 3.4-fold for *CD97* (see Figure 15A), 4.7-fold for *LRRC8A* (see Figure 15B), 22-fold for *SLC37A2* (see Figure 15C) and 3-fold for *NRIP1* (Figure 15D). While in PMA-differentiated cells the genes *LRRC8A* and *NRIP1* were already significantly up-regulated after 2 h, the genes *SLC37A2* and *CD97* reached this status only after 4 and 6 h, respectively. Moreover, in this cellular model the increase of gene expression after 24 h ligand stimulation was only 1.5-fold for *CD97* (see Figure 15A), 3.6-fold for *LRRC8A* (see Figure 15B), 2.5-fold for *SLC37A2* (see Figure 15C) and 2.2-fold for *NRIP1* (see Figure 15D). The overall weaker response of all four genes in PMA-differentiated cells shows no correlation to the changes of the basal expression of the genes, since during the differentiation process the genes *CD97* and *LRRC8A* reduced their expression 2.1- and 1.9-fold, while the genes *SLC37A2* and *NRIP1* increased their mRNA levels 3.9- and 1.3-fold (see Figure 16).

Taken together, in undifferentiated THP-1 cells the genes *CD97*, *LRRC8A*, *SLC37A2* and *NRIP1* are early responding 1,25(OH)$_2$D$_3$ targets with maximal inductions between 3- and 22-fold, while in PMA-differentiated cells the genes are less inducible and in part respond only delayed to the natural VDR ligand.

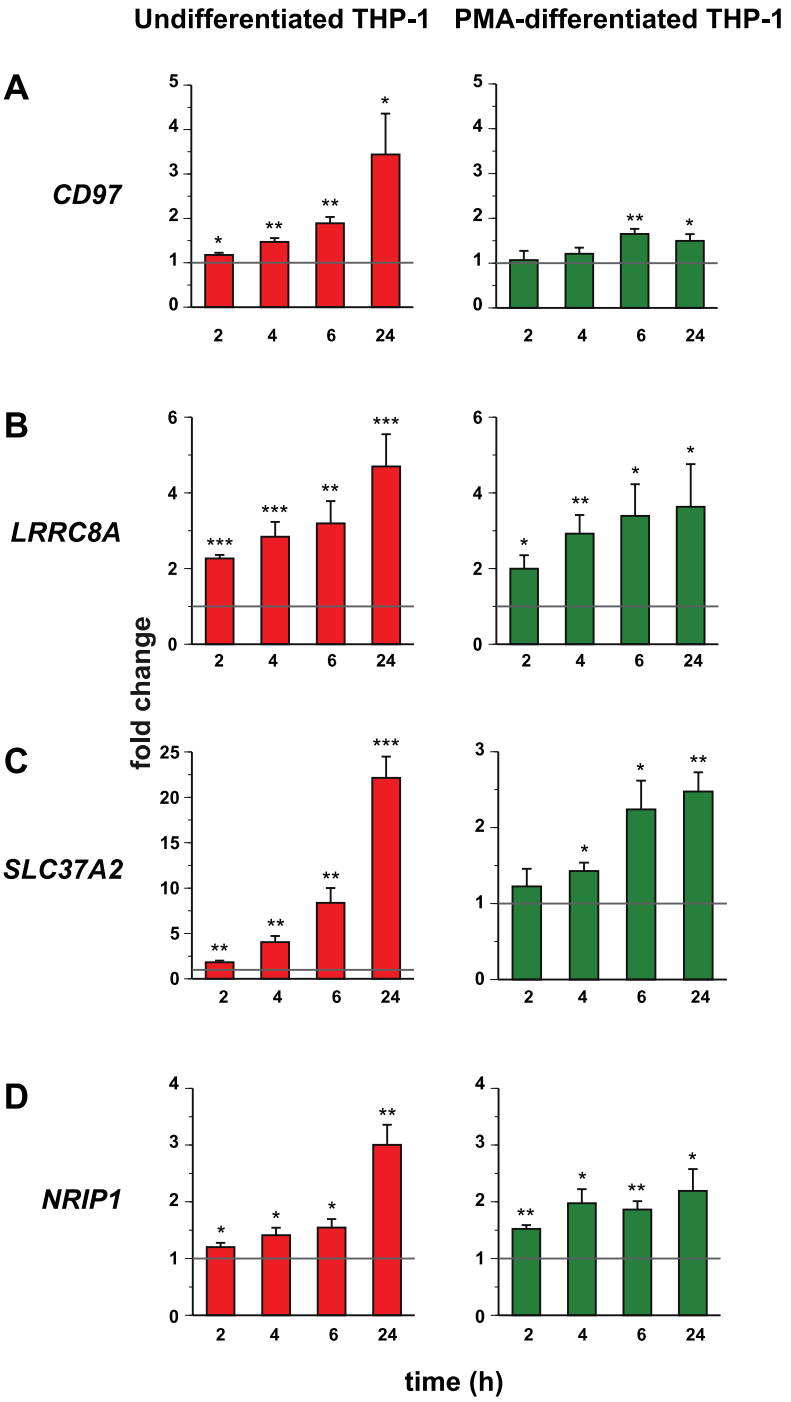

Figure 15: Expression profiling of primary VDR target genes. qPCR was performed to determine the relative changes of mRNA expression of the genes *CD97* (A), *LRRC8A* (B), *SLC37A2* (C) and *NRIP1* (D) normalized by the reference genes *B2M*, *GAPDH* and *HPRT1*. Undifferentiated (left) or PMA-differentiated THP-1 cells (right) were incubated with 100 nM $1,25(OH)_2D_3$ for either 2, 4, 6 or 24 h. The columns represent the means of three independent experiments (each performed in triplicate) and the bars indicate standard deviations. Two-tailed Student's t-tests were performed to determine the significance of the mRNA induction by $1,25(OH)_2D_3$ in reference to solvent-treated cells (* $p < 0.05$; ** $p < 0.01$; *** $p < 0.001$).

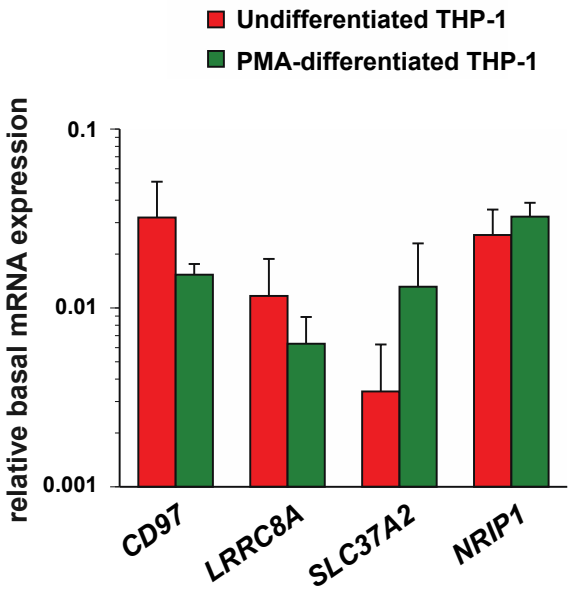

Figure 16: Basal mRNA expression of VDR target genes. In undifferentiated (red) and PMA-differentiated THP-1 cells (green). qPCR was performed to determine the relative basal expression of the genes *CD97*, *LRRC8A*, *SLC37A2* and *NRIP1* in relation to an average of the reference genes *B2M*, *GAPDH* and *HPRT1*. The columns represent the means of three independent experiments and the bars indicate standard deviations.

IV.V Response of VDR target genes in primary human samples

In order to evaluate the impact of the 1,25$(OH)_2D_3$ responsiveness of the genes *CD97*, *LRRC8A*, *SLC37A2* and *NRIP1* in primary human cells, we investigated the expression of these genes in PBMCs, which were isolated from participants of a vitamin D_3 intervention study (VitDmet, NCT01479933, ClinicalTrials.gov). This three-armed trial (placebo, 40 or 80 µg daily vitamin D_3 supplementation over 5 months) had recruited pre-diabetic (impaired fasting glucose or impaired glucose tolerance) human subjects from the region of Kuopio, Finland (63 °N) [104] and was performed during the winter season, where in the Northern hemisphere at this latitude, due to insufficient natural UV-B source, no vitamin D_3 was synthesized in the skin of the participants. The design of the study resulted in a large range of serum 25$(OH)D_3$ concentrations between 27.5 and 155.7 nM and changes ranging from a decrease by 30.2 nM and an increase by 87.2 nM. For further analysis we expressed these changes as ratios and not as differences, the 5-months intervention resulted in changes of the

serum 25(OH)D_3 concentrations ranging from a 2.1-fold decrease up to a 2.8-fold increase. In this way, the results of the 5-months intervention were interpreted in the same way as the cell culture ligand stimulation experiments (see Figure 15).

We used qPCR to measure the relative mRNA expression of primary VDR target genes in PBMCs of the 71 participants at the start and end of the intervention. For *NRIP1* we observed a range from a 1.45-fold decrease to a 1.77-fold increase, for *LRRC8A* from 1.45-fold decrease to 1.53-fold increase, for *SLC37A2* from 2.33-fold decrease to 3.05-fold increase and for *CD97* from 1.54-fold decrease to 1.87-fold increase. In previous studies[50,61,105] we had shown that the genes *THBD* and *CD14* are primary VDR targets and can serve as biomarkers for the vitamin D status of human individuals[96]. In the same PBMC samples the mRNA expression levels of *THBD* varied between a 1.94-fold down-regulation to a 1.89-fold up-regulation and *CD14* ranged from 1.79-fold down- to 1.94-fold up-regulation[96]. In addition, the six genes differed clearly in their mean relative basal expression, where *CD14* is 2-, 23-, 35-, 71-, and 105-times higher expressed than *CD97*, *NRIP1*, *LRRC8A*, *SLC37A2* and *THBD*, respectively (see Figure 17).

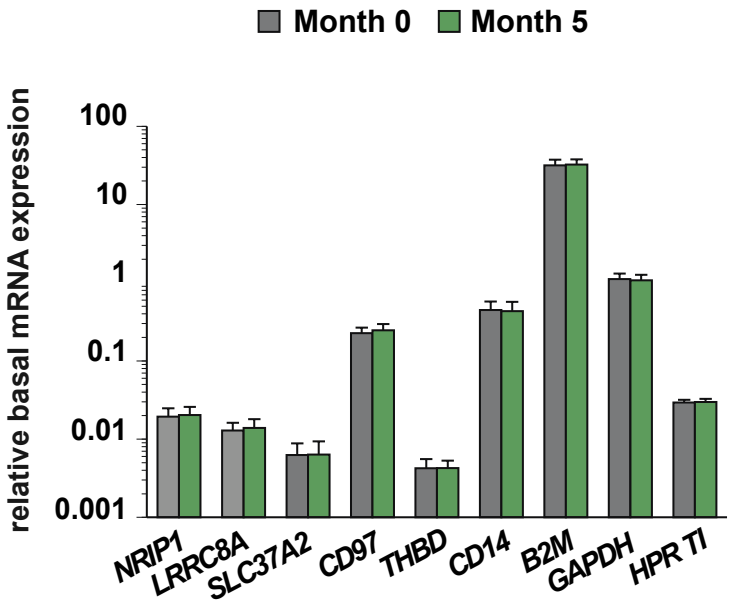

Figure 17: Basal mRNA expression in PBMCs. In PBMCs isolated from study participants before (grey) and after (green) the 5-months vitamin D intervention trial mRNA expression of the VDR target genes *CD97*, *LRRC8A*, *SLC37A2*, *NRIP1*, *THBD* and *CD14* and the reference genes *B2M*, *GAPDH* and *HPRT1* was determined by qPCR. The columns represent the means of all study participants and the bars indicate standard deviations.

Following the concepts of our previous study[96], we assumed a positive correlation between the expression changes of up-regulated primary VDR target genes and the respective alterations of serum 25(OH)D_3 concentrations during the intervention and used it for rankings of the study participants. Starting with all study participants, we omitted in the reverse order of the gene-specific ranking one participant after the other from the group. In case of equal ranks the participant with the higher ratio of gene expression change to serum 25(OH)D_3 concentration alteration was excluded first. After each omission we calculated the correlation coefficient r between the gene expression changes and the respective alterations in serum 25(OH)D_3 concentrations for the remaining participants. For each of the six genes the r-value was then plotted in relation to the number of study participants that were used for the respective calculation (see Figure 18 and 19). As expected, the r-values increased with smaller numbers of considered participants. However, the six genes showed individual differences. In order to obtain an r-value of 0.71 (which equals to a r^2-value of approximately 0.5) with the ranking based on *NRIP1* expression changes, only 30 of the 71 study participants needed to be eliminated, while for *LRRC8A* and *SLC37A2* each 35 and for *CD97* even 36 individuals had to be removed (see Figure 18). For comparison, in order to obtain the same r-values with *THBD*, 37 participants and with *CD14* even 43 individuals could not be considered[96] (see Figure 19).

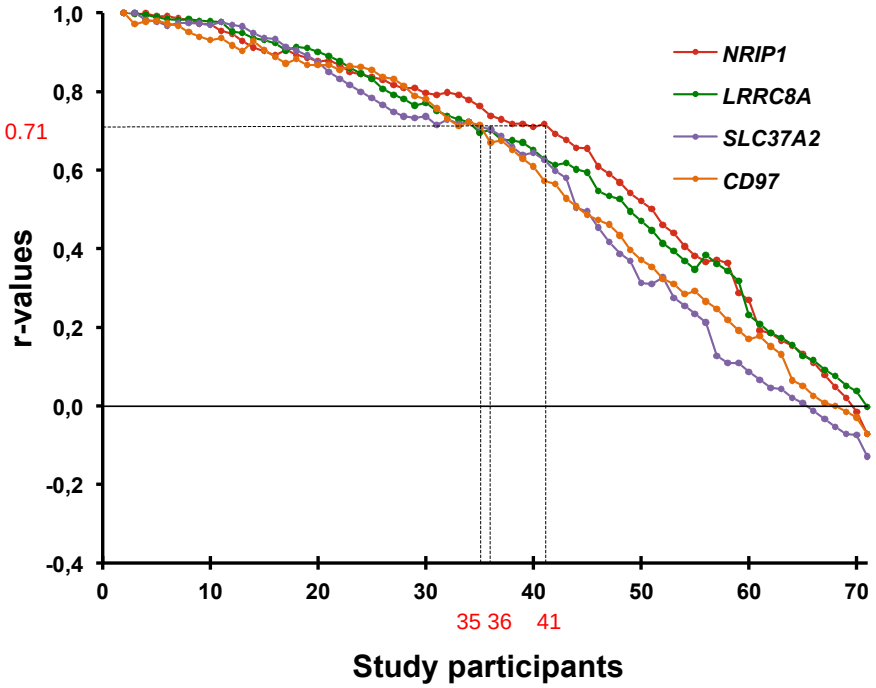

Figure 18: VDR target gene-specific ranking of vitamin D_3 intervention study participants. RNA was isolated from PBMCs obtained from 71 participants before and after a 5-months vitamin D_3 intervention trial. RT-qPCR was performed to determine the relative changes of the expression of the genes *NRIP1*, *LRRC8A*, *SLC37A2* and *CD97* normalized by the reference genes *B2M*, *GAPDH* and *HPRT1*. The study participants were ranked for the changes of the four VDR target genes in relation to changes in their 25(OH)D_3 serum levels. Starting from the lowest ranking participants the number of persons considered for correlation analysis were step-wise reduced and the respective r-values were plotted over the number of remaining subjects. The numbers of study participants that resulted in an r-value of 0.71 (r^2 = 0.5) are indicated in red. The respective correlation graphs are shown in Figures 20A-D.

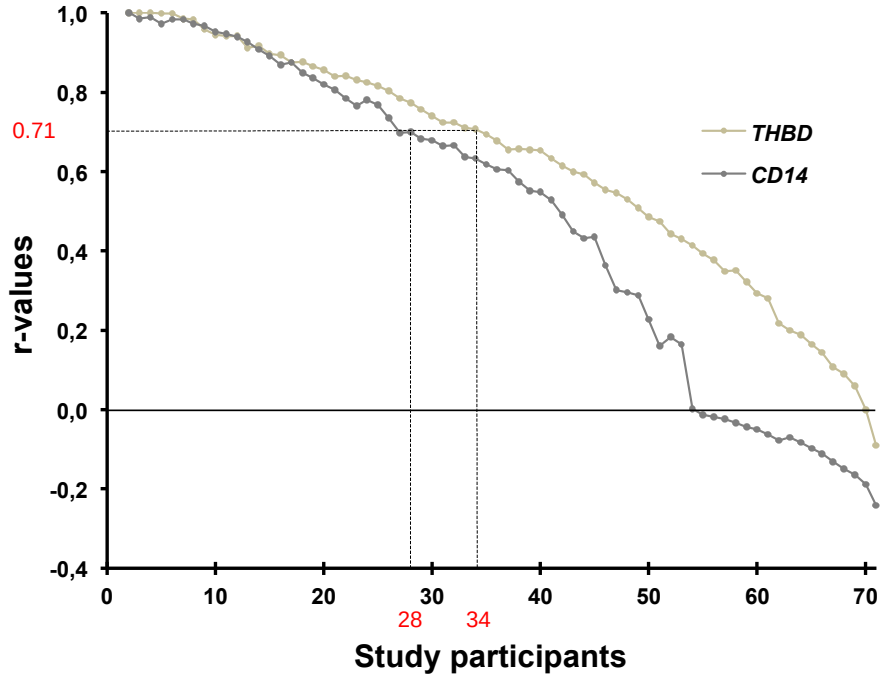

Figure 19: VDR target gene-specific ranking of vitamin D_3 intervention study participants. RNA was isolated from PBMCs obtained from 71 participants before and after a 5-months vitamin D_3 intervention trial. qPCR was performed to determine the relative changes of the expression of the VDR target genes *THBD* and *CD14* normalized by the reference genes *B2M*, *GAPDH* and *HPRT1*[96]. The study participants were ranked for the changes of gene expression in relation to alterations in their 25(OH)D_3 serum levels. Starting from the lowest ranking participants the number of persons considered for correlation analysis were step-wise reduced and the respective r-values were plotted over the number of remaining subjects. The numbers of study participants that resulted in an r-value of 0.71 (r^2 = 0.5) are indicated in red. The respective correlation graphs are shown in Figures 20E and F.

For illustrative purposes correlation graphs are shown for *NRIP1* (41 participants, Figure 20A), *LRRC8A* (36 participants, Figure 20B), *SLC37A2* (36 participants, Figure 20C), *CD97* (35 participants, Figure 20D), *THBD* (34 participants, Figure 20E) and *CD14* (28 participants, Figure 20F), which all showed an r^2-value in the order of 0.5. Red dots in these graphs indicate identical individuals. This indicates that with the exception of two subjects a ranking based on *NRIP1* expression described the same group of persons (and even 13 (46%) more) than the ranking based on expression of the previously published biomarker *CD14*[96,106].

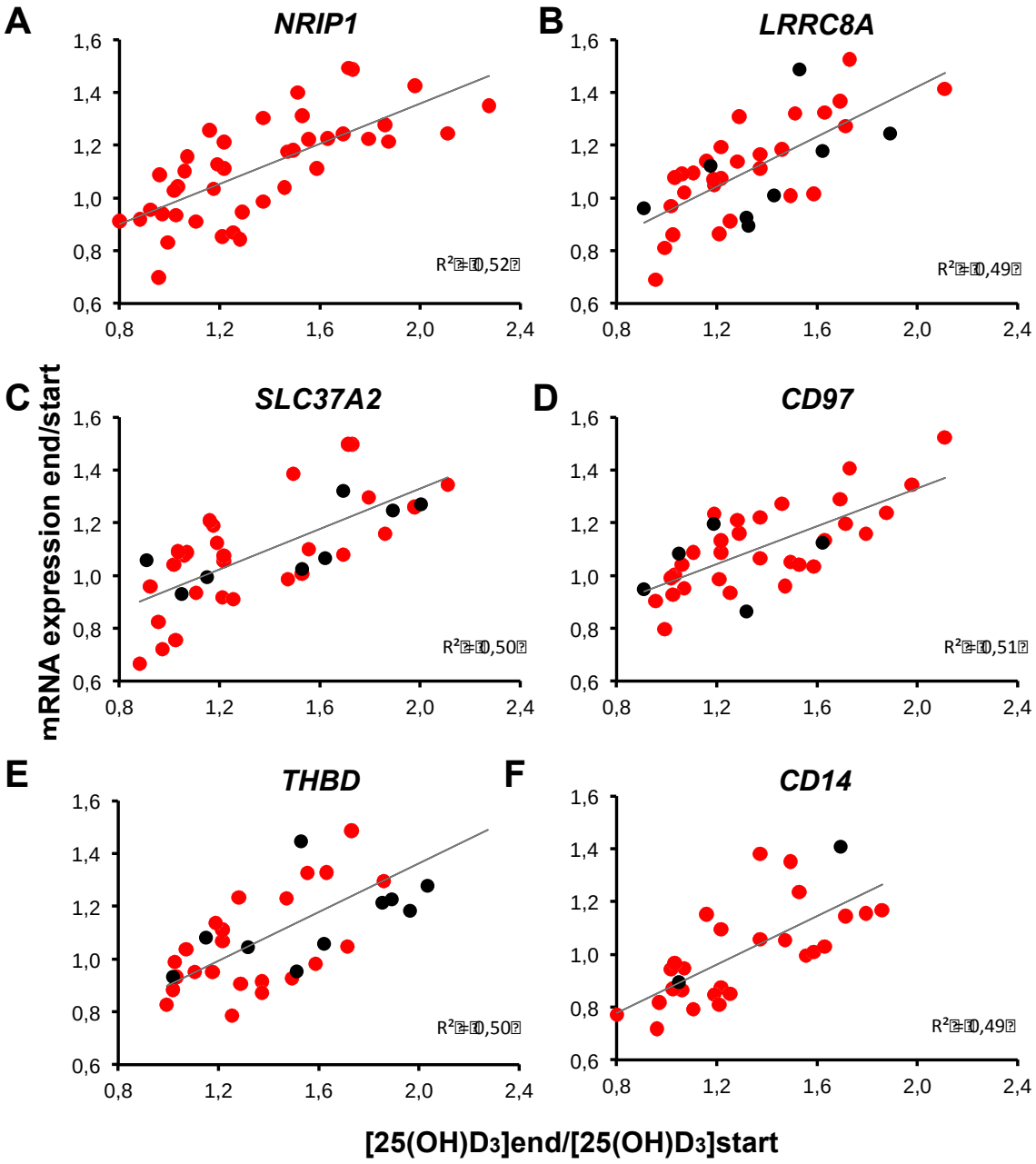

Figure 20: Changes in VDR target gene expression correlate with alterations in serum 25(OH)D_3 concentrations in PBMCs. The study participants were ranked for their changes of *NRIP1* (A), *LRRC8A* (B), *SLC37A2* (C), *CD97* (D), *THBD* (E) and *CD14* (F) mRNA expression in PBMCs in relation to serum 25(OH)D_3 concentrations. Starting from the lowest ranking participants the number of persons considered for correlation analysis were step-wise reduced. Here example graphs are shown, where r-values in the order of 0.71 were obtained (see Figures 18 and 19). Red dots indicate the 41 study participants that where top-ranked based on *NRIP1* mRNA expression, while black dots represent individuals outside of this group.

In summary, the new identified primary VDR target genes *NRIP1*, *LRRC8A*, *SLC37A2* and *CD97* can be used in primary human PBMCs, as biomarkers for the vitamin D status of human individuals. In particular, *NRIP1* seems to be well suited and exceeds the potential of the previously identified marker *CD14* by more than 40%.

V Discussion

In this study, we investigated four loci of the human genome, at which a prominent VDR binding site is co-located with a primary 1,25$(OH)_2D_3$ target gene. All four genes, *CD97*, *LRRC8A*, *SLC37A2* and *NRIP1*, had not been known before as targets of vitamin D. The proteins encoded by these genes represent rather divergent functions ranging from adhesion molecules (CD97[107] and LRRC8A[71]) via a glucose transporter (SLC37A2[72]) to a nuclear co-activator (NRIP1[75]). This re-emphasizes the pleiotropic actions of vitamin D, 1,25$(OH)_2D_3$, and the nuclear receptor VDR.

CD97 expression is increased after 1,25$(OH)_2D_3$ treatment in monocytes but not in macrophages. However, there also exists a correlation between *CD97* expression and diseases as for instance different cancers[62,68]. The ligand CD55/DAF seems to suppress the *CD97* expression and acts as a regulator of that gene. Besides that the binding of CD55/DAF to CD97 represses the complement system[64]. For that reason CD97 may act via its ligand more as a protection against cell damage.

LRRC8A expression is increased after 1,25$(OH)_2D_3$ treatment in both monocytes and macrophages. However, after macrophage differentiation with LPS LRRC8A mRNA expression is repressed[69]. *LRRC8A* is linked to B cell development and furthermore to adaptive immunity. It seems that the gene expression stimulation with 1,25$(OH)_2D_3$ influences the B cell maturation and therefore has a positive effect on the immune system. For further conclusions more knowledge is needed, especially in perspective on ligand identification.

SLC37A2 expression is increased after 1,25$(OH)_2D_3$ treatment in both monocytes and macrophages. However, the expression during macrophage differentiation increases as well[74]. It seems that this gene plays an important role in sugar metabolism especially in macrophages, which are located in the white adipose tissue[74]. This tissue plays a central role in the process and

development of inflammation and several diseases. For specific evidence how vitamin D is involved in this action further studies are needed.

NRIP1 expression is increased after 1,25$(OH)_2D_3$ treatment in both monocytes and macrophages. *NRIP1* acts as a co-repressor and co-activator for several nuclear receptors, especially in immune cells[75,76]. In contrast to the proteins encoded by all other investigated genes NRIP1 operates directly on the chromatin level[76]. The fact that 1,25$(OH)_2D_3$ stimulates the expression in both systems leads to its fine tuning functions with respect to innate immunity and inflammatory processes.

Undifferentiated and PMA-differentiated THP-1 cells represent two important cell types, monocytes and macrophages, of the myeloid lineage of the hematopoietic system. Three (*LRRC8A*, *SLC37A2* and *NRIP1*) of the four investigated genes are vitamin D targets in both cellular models and only the response of the *CD97* gene to 1,25$(OH)_2D_3$ is restricted to monocytic cells. Our observation that in PMA-differentiated THP-1 cells the chromatin at both $P1_{CD97}$ and $P2_{CD97}$ was not accessible and that therefore no VDR association at these sites could be detected, provides an obvious explanation why in these cells the *CD97* gene was not responsive to vitamin D_3. In turn, at the three other investigated major VDR binding sites ($P1_{LRRC8A}$, $P_{SLC37A2}$ and $P1_{NRIP1}$) also in PMA-differentiated THP-1 cells open chromatin and significant VDR binding could be detected, while in undifferentiated cells all four chromatin loci were accessible and VDR-bound. Interestingly, $P1_{LRRC8A}$, $P_{SLC37A2}$ and $P1_{NRIP1}$, but not $P1_{CD97}$, carry a DR3-type sequence below their summits. The latter sequences are known to be the preferred binding sites for VDR[41,108], but all published VDR ChIP-seq datasets[49-51] reported that the occurrence of DR3-type sequences at VDR loci is rather an exception than the rule. Since VDR heterodimerizes with RXRs preferentially on DR3-type sequences[41], at alternative DNA binding sequences the receptor most likely uses different dimerization partners or may even contact DNA only indirectly via binding "backpack" to another transcription factor[109].

Taken together, identifying a DR3-type sequence below a VDR peak summit is a strong indication for a major VDR binding site[61] and allows conclusions on the mechanism of VDR's function at this site.

The combination of i) a genome-wide monitoring of open chromatin via FAIRE-seq, ii) the assessment of genomic VDR binding via ChIP-seq and iii) a screening for DR3-type sequences below the peak summits is an efficient tool for the prediction and identification of primary $1,25(OH)_2D_3$ target genes. Interestingly, in all other publically accessible ChIP-seq datasets[49,51] the sites $P1_{LRRC8A}$, $P_{SLC37A2}$ and $P1_{NRIP1}$ are occupied by VDR (unpublished results), at least in B cells, colon and hepatic stellate cells the genes, which are controlled by these sites, should be primary VDR targets as well. In contrast, the site $P1_{CD97}$ is not recognized in ChIP-seq datasets of other cell types indicating that the $1,25(OH)_2D_3$ response of the *CD97* gene may be rather cell-type specific. Also it seems that loci with a DR3-sequence are isolated VDR binding sites in different tissues whereas such without a DR3 domain are not.

Higher-order genome structures, such as DNA looping, contribute to many nuclear functions, including the control of gene expression[110]. Moreover, large-scale genome-wide studies on transcription factor binding sites, chromatin modifications and accessible chromatin, such as provided by the ENCODE consortium[101], have indicated that the main regulatory sites of a gene can be far more than 100 kb up- or downstream of its TSS region. We could confirm this observation for the transcription factor VDR, where, for example, the major VDR binding site regulating *THBD* is 290 kb upstream of the gene's TSS[105]. Therefore, the size of the chromatin domain, which contains both the TSS and the major VDR binding site of a primary $1,25(OH)_2D_3$ target gene, is an important additional information for assessing the impact of a receptor-occupied VDR binding site for the regulation of its neighboring genes. From the four genomic loci investigated in this study, the genes *LRRC8A* and *SLC37A2* represent very obvious cases, where the major VDR binding sites are only 0.8 kb downstream and 7.5 kb upstream, respectively, of their gene's TSS. In

contrast, the major VDR sites of the genes *CD97* and *NRIP1* are with 56 and 158 kb far more distant from their respective TSS regions. Nevertheless, ChIA-PET data suggest that concerning all four investigated genes the respective chromatin domains are so large that they carry both the major VDR site and the respective TSS region. The chromatin loops of the genes *CD97*, *LRRC8A* and *NRIP1* contain in addition also minor VDR binding sites. $P2_{CD97}$ and $P2_{LRRC8A}$ were not statistically significant in ChIP-seq analysis. $P2_{CD97}$ shows open chromatin but no $1,25(OH)_2D_3$ effect. The presence of a CTCF site (Figure 14A, violet triangle) at the VDR peak explains the accessible chromatin. $P2_{LRRC8A}$ shows only weak chromatin opening and therefore most likely both sites do not contribute to the $1,25(OH)_2D_3$ responsiveness of *CD97* and *LRRC8A*. In contrast, $P2_{NRIP1}$ is not only in undifferentiated THP-1 but also in lymphoblastoid cells associated with VDR[49]. Moreover, this site carries a DR3-type binding sequence. Therefore, NRIP1 seems to belong to the smaller set of primary $1,25(OH)_2D_3$ target genes, which are controlled by two VDR sites. Interestingly, the *CD14* gene has a similar constellation with two VDR sites 24 and 26 kb downstream of its TSS region[61]. Thus, the likelihood that the ligand finds the receptor and furthermore regulates the gene is from a purely mathematical view higher.

Sufficient exposure to natural UV-B radiation or adequate intake from diet or supplements is needed to achieve an optimal serum $25(OH)D_3$ concentration. However, the change in serum $25(OH)D_3$ concentrations can vary widely from person to person. Diet and sun exposure together with age and adiposity in average account only for some 30% of the inter-individual variation in serum $25(OH)D_3$ concentrations[111]. Accordingly, genetic and epigenetic factors are responsible for the main variation in vitamin D concentrations[112-114]. Based on this wide inter-individual response variation, it is obvious that a “one-size-fits-all” approach will not work ideally for vitamin D_3 supplementation.

The fact that the *NRIP1* gene is controlled by two VDR sites may have some impact on its response to $1,25(OH)_2D_3$ and could be one reason, why the

expression of this gene seems to be a biomarker for the vitamin D_3 status that describes a larger subset of human individuals (57.7%) than *LRRC8A* (50.7%), *SLC37A2* (50.7%) or *CD97* (49.3%). Furthermore, in this study we used a far higher threshold (r^2 >0.49) for the correlation between gene expression changes and alterations in serum 25(OH)D_3 concentrations than in our previous report[96]. This means that for 41 of the 71 study participants the NRIP1 mRNA expression depends linearly on their serum 25(OH)D_3 concentration and these individuals are not yet saturated in their response to vitamin D and furthermore a vitamin D supplementation is reasonable.

In this study, we investigated the ranking of the VDR target genes individually and only in one tissue, while in our previous study[96] we combined the ranking based on two genes (*THBD* and *CD14*) in PBMCs and adipose tissue. Importantly, the ranking based on the best biomarker of this study (*NRIP1*) described, with exceptions of two participants, the same individuals as the best marker of our previous approach (*CD14*) and 13 additional subjects. This suggests that *NRIP1* may not only be a possible replacement for *CD14* as biomarker for the vitamin D status of human individuals but that it is also able to represent a larger proportion of the human population.

The PBMCs used in this study represent an easily available tissue, which would allow the screening of larger populations. However, the *NRIP1* gene is expressed in many human metabolic and reproductive tissues[115] and in all cell types, which were tested so far, the same set of two VDR binding sites are active. This indicates that the results which are obtained with *NRIP1* in PBMCs may be extrapolated to other tissues, such as colon and liver and that thus *NRIP1* could be used as a biomarker for the vitamin D_3 status also for other tissues. For 71 participants of the VitDmet trial the biomarker *NRIP1* indicates that the majority of them would benefit from a supplementation with vitamin D_3. Only 7 of these 41 top-ranked individuals had an initial serum 25(OH)D_3 concentration of below 50 nM, which according to Institute-of-Medicine recommendations[1], need to be supplemented by vitamin D_3. However, also the

other 34 responding individuals showed, on the level of the response of primary VDR target genes, a benefit from extra vitamin D_3. In contrast, 23 of the non-responsive 30 individuals had already at the start of the study a 25(OH)D_3 serum level above 50 nM, further vitamin D_3 supplementation may have been unnecessary. Alternatively, some of the non-responsive study participants may have a polymorphism in the VDR gene or in one of the genes encoding for vitamin D transporters or metabolizing enzymes[116,117], which may have diminished their response to vitamin D_3.

VI Conclusion

In conclusion, using a combination of genome-wide, molecular biology and bioinformatics approaches, we identified and characterized with *CD97*, *LRRC8A*, *SLC37A2* and *NRIP1* four novel primary 1,25$(OH)_2D_3$ target genes in monocyte- and macrophage-like cells. One of these genes, *NRIP1*, showed to be the presently known best molecular marker for the vitamin D status in the hematopoietic system.

VII Summary

The vitamin D endocrine system is not only involved in calcium and phosphate homeostasis and bone mineralization[11], but the fat-soluble vitamin also has anti-proliferative and immune-modulatory functions[42,118]. With energy provided by UV-B radiation 7-dehydrocholesterol converts in the skin to vitamin D_3[119], which is then metabolized into the widely accepted indicator of the vitamin D_3 status of the human body, 25(OH)D_3[120]. 1α-hydroxylation of 25(OH)D_3 into its hormonal form, 1,25(OH)2D_3, creates a specific high-affinity ligand of the transcription factor VDR[104]. VDR belongs to the unique transcription factor superfamily of nuclear receptors, whose members are directly activated by small lipophilic compounds[121].

Transcriptome-wide analysis indicated that per cell type between 200 and 600 genes are primary targets of vitamin D[32,49,50]. Undifferentiated THP-1 monocytic leukemia cells (monocytes) and PMA- differentiated THP-1 cells (M2-type macrophages) represent two important cell types of the myeloid lineage of the hematopoietic system. They represent a well responding and physiologically meaningful model system for the investigation of 1,25$(OH)_2D_3$ signaling in the context of innate immunity and cancer[32,50,109,122,123].

The human genome is organized into chromatin domains, in which gene regulatory events, such as the formation of physical connections between TSSs and transcription factor binding sites, are insulated from each other[124]. Most insulator regions between these chromatin domains are associated with the highly conserved transcription factor CTCF[36]. ChIA-PET[125] is used to assess the 3-dimensional organization of chromatin.

Genomic VDR binding sites are preferentially formed of a direct repeat of two hexameric binding motifs spaced by three nucleotides[126,127]. Ligand-activated VDR is linked by mediator proteins to the basal transcriptional machinery[32], which then results in transcriptional activation[128]. Like most other transcription factors, VDR competes with the intrinsic repressive nature of chromatin for

access to its genomic binding sites[28,53,129]. Open chromatin regions can be detected by the genome-wide method FAIRE-seq[31,33].

In this study, we used a combination of i) an assessment of chromatin loops containing a VDR binding site, ii) a genome-wide monitoring of open chromatin via FAIRE-seq, and iii) a screening for DR3-type sequences below VDR ChIP-seq peak summits as a tool for a classification of primary $1,25(OH)_2D_3$ target genes. As representatives for the functional diversity of these $1,25(OH)D_3$ targets, we selected the genes encoding for the adhesion molecules *CD97* and *LRRC8A*, the glucose transporter *SLC37A2* and the co-activator *NRIP1*. In undifferentiated THP-1 cells the VDR binding sites close to these four genes are associated with open chromatin and occupied by VDR, while in PMA-differentiated THP-1 cells only the sites of *LRRC8A*, *SLC37A2* and *NRIP1* are accessible and receptor-bound. We found *CD97*, *LRRC8A*, *SLC37A2* and *NRIP1* to be early responding $1,25(OH)_2D_3$ target genes in monocytic cells, while in macrophage-like cells they respond less and in part delayed. Most importantly, in human PBMCs all four genes can be used as transcriptomic biomarkers to classify human individuals for their possible benefit from a vitamin D_3 supplementation. In particular, *NRIP1* exceeds the potential of the previously identified marker *CD14* by more than 40% and presently seems to be the best molecular marker for the vitamin D_3 status in the hematopoietic system.

VIII Zusammenfassung

Vitamin D gehört zu den fettlöslichen Vitaminen und hat einen wichtigen Einfluss auf die Regulation der Calcium-Phosphat Homöostase und beeinflusst somit die Knochenmineralisierung[11]. Gegenwärtig nehmen antiproliferative und immunomodulatorische Aspekte von Vitamin D immer mehr an Bedeutung zu[42,118]. In der Haut wird 7-Dehydrocholesterol, unter Energiebereitstellung von UV-B Strahlen, zu Vitamin D_3 synthetisiert[119] und weiter zu 25(OH)D_3 metabolisiert. Letzteres stellt einen anerkannten Indikator für den Vitamin D_3 Status im menschlichen Körper dar und durch 1α-Hydroxylierung entsteht 1,25$(OH)_2D_3$, der spezifische hochaffine Ligand des Transkriptionsfaktors VDR[104,120]. VDR zählt zu den nuklearen Rezeptoren und wird durch kleine lipophile Substanzen aktiviert[121].
Transkriptomweite Analysen weisen darauf hin, dass pro Zelltyp zwischen 200 und 600 Gene von Vitamin D beeinflusst und reguliert werden[32,49,50]. Undifferenzierte THP-1 Zellen (Monozyten) und PMA- differenzierte THP-1 Zellen (M2-Typ Makrophagen) stellen zwei wichtige Typen des hämatopoetischen Systems dar. Sie repräsentieren ein physiologisch aussagekräftiges System für die Untersuchung von 1,25$(OH)_2D_3$ im Zusammenhang mit dem angeborenen Immunsystem und Krebs[32,50,109,122,123].

Das menschliche Genome ist in Chromatin-Domänen organisiert, in denen genregulatorische Aktivitäten, wie zum Beispiel die Verbindung von TSSs und Transkriptionsfaktoren, isoliert vorliegen[124]. Die meisten Isolatorbereiche sind mit dem Transkriptionsfaktor CTCF[36] verbunden und die 3-dimensionale Organisation des Chromatins kann durch ChIA-PET[125] Analysen beurteilt werden.

Die bevorzugte genomische VDR Bildungsstelle setzte sich aus zwei Wiederholungen von je sechs Nukleotiden zusammen, mit einem Abstand von drei Nukleotiden[126,127]. Bindet der Ligand an VDR wird dieser aktiviert und mit dem basalen Transkriptionsapparat verbunden, was zur Transkription führt[32,128].

Dazu ist geöffnetes Chromatin notwendig, welches durch die Analyse mit FAIRE identifiziert und untersucht werden kann[28,31,33,53,129].

In dieser Studie wurde eine Kombination aus i) einer Bewertung von VDR Bindungsstellen innerhalb eines loops, ii) einer Beurteilung von offenem Chromatin mittels FAIRE-seq und iii) einem Screening für DR3 Sequenzen unter VDR ChIP-seq Peaks als Hilfestellung für eine Einstufung von primären $1,25(OH)_2D_3$ Genen verwendet. Die Gene kodierend für die Adhäsionsmoleküle *CD97* und *LRRC8A*, den Glucose Transporter *SLC37A2* und den Co-Aktivator *NRIP1* repräsentieren die Funktionalität und Diversität von Vitamin D. In undifferenzierten THP-1 Zellen sind die VDR Bindungsstellen aller vier Gene besetzt und mit offenem Chromatin assoziiert. In PMA-differenzierten THP-1 Zellen sind nur die Gene *LRRC8A*, *SLC37A2* und *NRIP1* zugänglich und mit VDR besetzt. In Monozyten reagieren alle vier Gene sehr früh auf eine $1,25(OH)_2D_3$ Zugabe, wohingegen in Makrophagen die Reaktion nicht so stark ausfiel und teilweise verzögert. Wesentlich ist die Erkenntnis, dass alle vier Gene in menschlichen PBMCs als Transkriptombiomarker verwendet werden können um einen möglichen Vorteil einer Vitamin D Supplementation zu identifizieren. Insbesondere *NRIP1* übertrifft das Potential des zuvor identifizierten Markers *CD14* um mehr als 40% und repräsentiert gegenwärtig den besten molekularen Marker für den Vitamin D_3 Status im hämatopoetischen System.

IX References

1. Institute of Medicine (US) Committee to Review Dietary Reference Intakes for Vitamin D and Calcium. 2011.

2. Reichrath J. Skin cancer prevention and UV-protection: How to avoid vitamin D-deficiency? *Br J Dermatol*. 2009;161 Suppl 3:54-60.

3. Holick MF, MacLaughlin JA, Clark MB, et al. Photosynthesis of previtamin D_3 in human skin and the physiologic consequences. *Science*. 1980;210(4466):203-205.

4. Zittermann A, Gummert JF. Nonclassical vitamin D action. *Nutrients*. 2010;2(4):408-425.

5. Vieth R. Vitamin D and cancer mini-symposium: The risk of additional vitamin D. *Ann Epidemiol*. 2009;19(7):441-445.

6. Aloia JF, Patel M, Dimaano R, et al. Vitamin D intake to attain a desired serum 25-hydroxyvitamin D concentration. *Am J Clin Nutr*. 2008;87(6):1952-1958.

7. Zittermann A. Vitamin D in preventive medicine: Are we ignoring the evidence? *Br J Nutr*. 2003;89(5):552-572.

8. Rosenstreich SJ, Rich C, Volwiler W. Deposition in and release of vitamin D_3 from body fat: Evidence for a storage site in the rat. *J Clin Invest*. 1971;50(3):679-687.

9. Schauber J, Dorschner RA, Coda AB, et al. Injury enhances TLR2 function and antimicrobial peptide expression through a vitamin D-dependent mechanism. *J Clin Invest*. 2007;117(3):803-811.

10. Holick MF. Vitamin D deficiency. *N Engl J Med*. 2007;357(3):266-281.

11. DeLuca HF. Overview of general physiologic features and functions of vitamin D. *Am J Clin Nutr*. 2004;80(6 Suppl):1689S-96S.

12. Holick MF. Vitamin D: Importance in the prevention of cancers, type 1 diabetes, heart disease, and osteoporosis. *Am J Clin Nutr*. 2004;79(3):362-371.

13. Haider N, Nagi AG, Khan KM. Frequency of nutritional rickets in children admitted with severe pneumonia. *J Pak Med Assoc*. 2010;60(9):729-732.

14. Hewison M, Freeman L, Hughes SV, et al. Differential regulation of vitamin D receptor and its ligand in human monocyte-derived dendritic cells. *J Immunol*. 2003;170(11):5382-5390.

15. Liu PT, Stenger S, Li H, et al. Toll-like receptor triggering of a vitamin D-mediated human antimicrobial response. *Science*. 2006;311(5768):1770-1773.

16. Adams JS, Hewison M. Unexpected actions of vitamin D: New perspectives on the regulation of innate and adaptive immunity. *Nat Clin Pract Endocrinol Metab*. 2008;4(2):80-90.

17. O'Brien MA, Jackson MW. Vitamin D and the immune system: Beyond rickets. *Vet J*. 2012;194(1):27-33.

18. Chavez-Sanchez L, Espinosa-Luna JE, Chavez-Rueda K, Legorreta-Haquet MV, Montoya-Diaz E, Blanco-Favela F. Innate immune system cells in atherosclerosis. *Arch Med Res*. 2014;45(1):1-14.

19. Ziegler-Heitbrock HW. Definition of human blood monocytes. *J Leukoc Biol*. 2000;67(5):603-606.

20. Tacke F, Randolph GJ. Migratory fate and differentiation of blood monocyte subsets. *Immunobiology*. 2006;211(6-8):609-618.

21. Murray PJ, Wynn TA. Protective and pathogenic functions of macrophage subsets. *Nat Rev Immunol*. 2011;11(11):723-737.

22. Oliver P, Reynes B, Caimari A, Palou A. Peripheral blood mononuclear cells: A potential source of homeostatic imbalance markers associated with obesity development. *Pflugers Arch*. 2013;465(4):459-468.

23. Caimari A, Oliver P, Rodenburg W, Keijer J, Palou A. Feeding conditions control the expression of genes involved in sterol metabolism in peripheral blood mononuclear cells of normoweight and diet-induced (cafeteria) obese rats. *J Nutr Biochem*. 2010;21(11):1127-1133.

24. Scherrer K, Jost J. Gene and genon concept: Coding versus regulation. A conceptual and information-theoretic analysis of genetic storage and expression in the light of modern molecular biology. *Theory Biosci*. 2007;126(2-3):65-113.

25. Scherrer K, Jost J. The gene and the genon concept: A functional and information-theoretic analysis. *Mol Syst Biol*. 2007;3:87.

26. Scherrer K. Regulation of gene expression and the transcription factor cycle hypothesis. *Biochimie*. 2012;94(4):1057-1068.

27. Orlando V. Mapping chromosomal proteins in vivo by formaldehyde-crosslinked-chromatin immunoprecipitation. *Trends Biochem Sci*. 2000;25(3):99-104.

28. Eberharter A, Becker PB. Histone acetylation: A switch between repressive and permissive chromatin. second in review series on chromatin dynamics. *EMBO Rep*. 2002;3(3):224-229.

29. Cockerill PN. Structure and function of active chromatin and DNase I hypersensitive sites. *FEBS J*. 2011;278(13):2182-2210.

30. Hayes JJ, Hansen JC. Nucleosomes and the chromatin fiber. *Curr Opin Genet Dev*. 2001;11(2):124-129.

31. Song L, Zhang Z, Grasfeder LL, et al. Open chromatin defined by DNaseI and FAIRE identifies regulatory elements that shape cell-type identity. *Genome Res*. 2011;21(10):1757-1767.

32. Carlberg C, Campbell MJ. Vitamin D receptor signaling mechanisms: Integrated actions of a well-defined transcription factor. *Steroids*. 2013;78(2):127-136.

33. Giresi PG, Lieb JD. Isolation of active regulatory elements from eukaryotic chromatin using FAIRE (formaldehyde assisted isolation of regulatory elements). *Methods*. 2009;48(3):233-239.

34. Li G, Fullwood MJ, Xu H, et al. ChIA-PET tool for comprehensive chromatin interaction analysis with paired-end tag sequencing. *Genome Biol*. 2010;11(2):R22-2010-11-2-r22. Epub 2010 Feb 25.

35. Handoko L, Xu H, Li G, et al. CTCF-mediated functional chromatin interactome in pluripotent cells. *Nat Genet*. 2011;43(7):630-638.

36. Schmidt D, Schwalie PC, Wilson MD, et al. Waves of retrotransposon expansion remodel genome organization and CTCF binding in multiple mammalian lineages. *Cell*. 2012;148(1-2):335-348.

37. Vaquerizas JM, Kummerfeld SK, Teichmann SA, Luscombe NM. A census of human transcription factors: Function, expression and evolution. *Nat Rev Genet*. 2009;10(4):252-263.

38. Mangelsdorf DJ, Thummel C, Beato M, et al. The nuclear receptor superfamily: The second decade. *Cell*. 1995;83(6):835-839.

39. Molnar F, Perakyla M, Carlberg C. Vitamin D receptor agonists specifically modulate the volume of the ligand-binding pocket. *J Biol Chem*. 2006;281(15):10516-10526.

40. Nagy L, Schwabe JW. Mechanism of the nuclear receptor molecular switch. *Trends Biochem Sci*. 2004;29(6):317-324.

41. Carlberg C, Bendik I, Wyss A, et al. Two nuclear signalling pathways for vitamin D. *Nature*. 1993;361(6413):657-660.

42. Verstuyf A, Carmeliet G, Bouillon R, Mathieu C. Vitamin D: A pleiotropic hormone. *Kidney Int*. 2010;78(2):140-145.

43. Polly P, Herdick M, Moehren U, Baniahmad A, Heinzel T, Carlberg C. VDR-alien: A novel, DNA-selective vitamin D_3 receptor-corepressor partnership. *FASEB J*. 2000;14(10):1455-1463.

44. Talbert PB, Henikoff S. Spreading of silent chromatin: Inaction at a distance. *Nat Rev Genet*. 2006;7(10):793-803.

45. Narlikar GJ, Fan HY, Kingston RE. Cooperation between complexes that regulate chromatin structure and transcription. *Cell*. 2002;108(4):475-487.

46. Xu L, Glass CK, Rosenfeld MG. Coactivator and corepressor complexes in nuclear receptor function. *Curr Opin Genet Dev*. 1999;9(2):140-147.

47. Glass CK, Rosenfeld MG. The coregulator exchange in transcriptional functions of nuclear receptors. *Genes Dev*. 2000;14(2):121-141.

48. Leo C, Chen JD. The SRC family of nuclear receptor coactivators. *Gene*. 2000;245(1):1-11.

49. Ramagopalan SV, Heger A, Berlanga AJ, et al. A ChIP-seq defined genome-wide map of vitamin D receptor binding: Associations with disease and evolution. *Genome Res*. 2010;20(10):1352-1360.

50. Heikkinen S, Vaisanen S, Pehkonen P, Seuter S, Benes V, Carlberg C. Nuclear hormone 1alpha,25-dihydroxyvitamin D_3 elicits a genome-wide shift in the locations of VDR chromatin occupancy. *Nucleic Acids Res*. 2011;39(21):9181-9193.

51. Meyer MB, Goetsch PD, Pike JW. VDR/RXR and TCF4/beta-catenin cistromes in colonic cells of colorectal tumor origin: Impact on c-FOS and c-MYC gene expression. *Mol Endocrinol*. 2012;26(1):37-51.

52. Ding N, Yu RT, Subramaniam N, et al. A vitamin D receptor/SMAD genomic circuit gates hepatic fibrotic response. *Cell*. 2013;153(3):601-613.

53. Carlberg C, Seuter S, Heikkinen S. The first genome-wide view of vitamin D receptor locations and their mechanistic implications. *Anticancer Res*. 2012;32(1):271-282.

54. Earnest C, Cooper KH, Marks A, Mitchell TL. Efficacy of a complex multivitamin supplement. *Nutrition*. 2002;18(9):738-742.

55. Hathcock JN, Shao A, Vieth R, Heaney R. Risk assessment for vitamin D. *Am J Clin Nutr*. 2007;85(1):6-18.

56. Vieth R. Critique of the considerations for establishing the tolerable upper intake level for vitamin D: Critical need for revision upwards. *J Nutr*. 2006;136(4):1117-1122.

57. Gallagher JC, Sai A, Templin T,2nd, Smith L. Dose response to vitamin D supplementation in postmenopausal women: A randomized trial. *Ann Intern Med*. 2012;156(6):425-437.

58. Zhao LJ, Zhou Y, Bu F, et al. Factors predicting vitamin D response variation in non-hispanic white postmenopausal women. *J Clin Endocrinol Metab*. 2012;97(8):2699-2705.

59. Berk M, Sanders KM, Pasco JA, et al. Vitamin D deficiency may play a role in depression. *Med Hypotheses*. 2007;69(6):1316-1319.

60. Pipingas A, Camfield DA, Stough C, et al. The effects of multivitamin supplementation on mood and general well-being in healthy young adults. A laboratory and at-home mobile phone assessment. *Appetite*. 2013;69:123-136.

61. Seuter S, Pehkonen P, Heikkinen S, Carlberg C. Dynamics of 1alpha,25-dihydroxyvitamin D_3-dependent chromatin accessibility of early vitamin D receptor target genes. *Biochim Biophys Acta*. 2013;1829(12):1266-1275.

62. Kwakkenbos MJ, Kop EN, Stacey M, et al. The EGF-TM7 family: A postgenomic view. *Immunogenetics*. 2004;55(10):655-666.

63. Gray JX, Haino M, Roth MJ, et al. CD97 is a processed, seven-transmembrane, heterodimeric receptor associated with inflammation. *J Immunol*. 1996;157(12):5438-5447.

64. Karpus ON, Veninga H, Hoek RM, et al. Shear stress-dependent downregulation of the adhesion-G protein-coupled receptor CD97 on circulating leukocytes upon contact with its ligand CD55. *J Immunol*. 2013;190(7):3740-3748.

65. Sutavani RV, Bradley RG, Ramage JM, Jackson AM, Durrant LG, Spendlove I. CD55 costimulation induces differentiation of a discrete T regulatory type 1 cell population with a stable phenotype. *J Immunol*. 2013;191(12):5895-5903.

66. Abbott RJ, Spendlove I, Roversi P, et al. Structural and functional characterization of a novel T cell receptor co-regulatory protein complex, CD97-CD55. *J Biol Chem*. 2007;282(30):22023-22032.

67. Visser L, de Vos AF, Hamann J, et al. Expression of the EGF-TM7 receptor CD97 and its ligand CD55 (DAF) in multiple sclerosis. *J Neuroimmunol*. 2002;132(1-2):156-163.

68. Steinert M, Wobus M, Boltze C, et al. Expression and regulation of CD97 in colorectal carcinoma cell lines and tumor tissues. *Am J Pathol*. 2002;161(5):1657-1667.

69. Kubota K, Kim JY, Sawada A, et al. LRRC8 involved in B cell development belongs to a novel family of leucine-rich repeat proteins. *FEBS Lett*. 2004;564(1-2):147-152.

70. Sawada A, Takihara Y, Kim JY, et al. A congenital mutation of the novel gene LRRC8 causes agammaglobulinemia in humans. *J Clin Invest*. 2003;112(11):1707-1713.

71. Abascal F, Zardoya R. LRRC8 proteins share a common ancestor with pannexins, and may form hexameric channels involved in cell-cell communication. *Bioessays*. 2012;34(7):551-560.

72. Pan CJ, Chen SY, Jun HS, Lin SR, Mansfield BC, Chou JY. SLC37A1 and SLC37A2 are phosphate-linked, glucose-6-phosphate antiporters. *PLoS One*. 2011;6(9):e23157.

73. Bartoloni L, Antonarakis SE. The human sugar-phosphate/phosphate exchanger family SLC37. *Pflugers Arch*. 2004;447(5):780-783.

74. Kim JY, Tillison K, Zhou S, Wu Y, Smas CM. The major facilitator superfamily member Slc37a2 is a novel macrophage- specific gene selectively expressed in obese white adipose tissue. *Am J Physiol Endocrinol Metab*. 2007;293(1):E110-20.

75. Nautiyal J, Christian M, Parker MG. Distinct functions for RIP140 in development, inflammation, and metabolism. *Trends Endocrinol Metab*. 2013;24(9):451-459.

76. Chung HT. RIP140, a janus metabolic switch involved in defense functions. *Cell Mol Immunol*. 2013;10(1):7-9.

77. Ho PC, Wei LN. Biological activities of receptor-interacting protein 140 in adipocytes and metabolic diseases. *Curr Diabetes Rev*. 2012;8(6):452-457.

78. Chao TH, Tsai WC, Chen JY, et al. Soluble thrombomodulin is a paracrine anti-apoptotic factor for vascular endothelial protection. *Int J Cardiol*. 2014;172(2):340-349.

79. Salomaa V, Matei C, Aleksic N, et al. Soluble thrombomodulin as a predictor of incident coronary heart disease and symptomless carotid artery

atherosclerosis in the atherosclerosis risk in communities (ARIC) study: A case-cohort study. *Lancet*. 1999;353(9166):1729-1734.

80. Esmon CT. The roles of protein C and thrombomodulin in the regulation of blood coagulation. *J Biol Chem*. 1989;264(9):4743-4746.

81. Asakura H, Takahashi H, Tsuji H, et al. Post-marketing surveillance of thrombomodulin alfa, a novel treatment of disseminated intravascular coagulation - safety and efficacy in 1,032 patients with hematologic malignancy. *Thromb Res*. 2014;133(3):364-370.

82. Zhang Y, Weiler-Guettler H, Chen J, et al. Thrombomodulin modulates growth of tumor cells independent of its anticoagulant activity. *J Clin Invest*. 1998;101(7):1301-1309.

83. Ulevitch RJ, Tobias PS. Receptor-dependent mechanisms of cell stimulation by bacterial endotoxin. *Annu Rev Immunol*. 1995;13:437-457.

84. Anas A, van der Poll T, de Vos AF. Role of CD14 in lung inflammation and infection. *Crit Care*. 2010;14(2):209.

85. Yang RB, Mark MR, Gurney AL, Godowski PJ. Signaling events induced by lipopolysaccharide-activated toll-like receptor 2. *J Immunol*. 1999;163(2):639-643.

86. Landmann R, Muller B, Zimmerli W. CD14, new aspects of ligand and signal diversity. *Microbes Infect*. 2000;2(3):295-304.

87. Estruch M, Bancells C, Beloki L, Sanchez-Quesada JL, Ordonez-Llanos J, Benitez S. CD14 and TLR4 mediate cytokine release promoted by electronegative LDL in monocytes. *Atherosclerosis*. 2013;229(2):356-362.

88. Wang R, Li KM, Zhou CH, Xue JL, Ji CN, Chen JZ. Cdc20 mediates D-box-dependent degradation of Sp100. *Biochem Biophys Res Commun*. 2011;415(4):702-706.

89. Wasylyk C, Schlumberger SE, Criqui-Filipe P, Wasylyk B. Sp100 interacts with ETS-1 and stimulates its transcriptional activity. *Mol Cell Biol*. 2002;22(8):2687-2702.

90. Moller A, Sirma H, Hofmann TG, et al. Sp100 is important for the stimulatory effect of homeodomain-interacting protein kinase-2 on p53-dependent gene expression. *Oncogene*. 2003;22(54):8731-8737.

91. Newhart A, Negorev DG, Rafalska-Metcalf IU, Yang T, Maul GG, Janicki SM. Sp100A promotes chromatin decondensation at a cytomegalovirus-promoter-regulated transcription site. *Mol Biol Cell*. 2013;24(9):1454-1468.

92. Tsuchiya S, Yamabe M, Yamaguchi Y, Kobayashi Y, Konno T, Tada K. Establishment and characterization of a human acute monocytic leukemia cell line (THP-1). *Int J Cancer*. 1980;26(2):171-176.

93. Mills CD. M1 and M2 macrophages: Oracles of health and disease. *Crit Rev Immunol*. 2012;32(6):463-488.

94. Livak KJ, Schmittgen TD. Analysis of relative gene expression data using real-time quantitative PCR and the $2^{-\text{delta delta } C_T}$ method. *Methods*. 2001;25(4):402-408.

95. Vandesompele J, De Preter K, Pattyn F, et al. Accurate normalization of real-time quantitative RT-PCR data by geometric averaging of multiple internal control genes. *Genome Biol*. 2002;3(7):RESEARCH0034.

96. Carlberg C, Seuter S, de Mello VD, et al. Primary vitamin D target genes allow a categorization of possible benefits of vitamin D_3 supplementation. *PLoS One*. 2013;8(7):e71042.

97. Nurmi T, Tuomainen TP, Virtanen J, Mursu J, Voutilainen S. High-performance liquid chromatography and coulometric electrode array detector in serum 25-hydroxyvitamin D_3 and 25-hydroxyvitamin D_2 analyses. *Anal Biochem*. 2013;435(1):1-9.

98. de Mello VD, Erkkila AT, Schwab US, et al. The effect of fatty or lean fish intake on inflammatory gene expression in peripheral blood mononuclear cells of patients with coronary heart disease. *Eur J Nutr*. 2009;48(8):447-455.

99. Thorvaldsdottir H, Robinson JT, Mesirov JP. Integrative genomics viewer (IGV): High-performance genomics data visualization and exploration. *Brief Bioinform*. 2013;14(2):178-192.

100. Kent WJ, Sugnet CW, Furey TS, et al. The human genome browser at UCSC. *Genome Res*. 2002;12(6):996-1006.

101. ENCODE Project Consortium, Bernstein BE, Birney E, et al. An integrated encyclopedia of DNA elements in the human genome. *Nature*. 2012;489(7414):57-74.

102. Klein E, Ben-Bassat H, Neumann H, et al. Properties of the K562 cell line, derived from a patient with chronic myeloid leukemia. *Int J Cancer*. 1976;18(4):421-431.

103. Phillips JE, Corces VG. CTCF: Master weaver of the genome. *Cell*. 2009;137(7):1194-1211.

104. Carlberg C, Molnar F. Current status of vitamin D signaling and its therapeutic applications. *Curr Top Med Chem*. 2012;12(6):528-547.

105. Seuter S, Heikkinen S, Carlberg C. Chromatin acetylation at transcription start sites and vitamin D receptor binding regions relates to effects of 1alpha,25-dihydroxyvitamin D_3 and histone deacetylase inhibitors on gene expression. *Nucleic Acids Res*. 2013;41(1):110-124.

106. Standahl Olsen K, Rylander C, Brustad M, Aksnes L, Lund E. Plasma 25 hydroxyvitamin D level and blood gene expression profiles: A cross-sectional study of the norwegian women and cancer post-genome cohort. *Eur J Clin Nutr*. 2013;67(7):773-778.

107. Hamann J, Veninga H, de Groot DM, et al. CD97 in leukocyte trafficking. *Adv Exp Med Biol*. 2010;706:128-137.

108. Umesono K, Murakami KK, Thompson CC, Evans RM. Direct repeats as selective response elements for the thyroid hormone, retinoic acid, and vitamin D_3 receptors. *Cell*. 1991;65(7):1255-1266.

109. FANTOM Consortium, Suzuki H, Forrest AR, et al. The transcriptional network that controls growth arrest and differentiation in a human myeloid leukemia cell line. *Nat Genet*. 2009;41(5):553-562.

110. Misteli T. Beyond the sequence: Cellular organization of genome function. *Cell*. 2007;128(4):787-800.

111. Engelman CD, Meyers KJ, Iyengar SK, et al. Vitamin D intake and season modify the effects of the GC and CYP2R1 genes on 25-hydroxyvitamin D concentrations. *J Nutr*. 2013;143(1):17-26.

112. Engelman CD, Fingerlin TE, Langefeld CD, et al. Genetic and environmental determinants of 25-hydroxyvitamin D and 1,25-dihydroxyvitamin D levels in hispanic and african americans. *J Clin Endocrinol Metab*. 2008;93(9):3381-3388.

113. Orton SM, Morris AP, Herrera BM, et al. Evidence for genetic regulation of vitamin D status in twins with multiple sclerosis. *Am J Clin Nutr*. 2008;88(2):441-447.

114. Snellman G, Melhus H, Gedeborg R, et al. Seasonal genetic influence on serum 25-hydroxyvitamin D levels: A twin study. *PLoS One*. 2009;4(11):e7747.

115. Steel JH, White R, Parker MG. Role of the RIP140 corepressor in ovulation and adipose biology. *J Endocrinol*. 2005;185(1):1-9.

116. Wang TJ, Zhang F, Richards JB, et al. Common genetic determinants of vitamin D insufficiency: A genome-wide association study. *Lancet*. 2010;376(9736):180-188.

117. Dastani Z, Li R, Richards B. Genetic regulation of vitamin D levels. *Calcif Tissue Int*. 2013;92(2):106-117.

118. Ingraham BA, Bragdon B, Nohe A. Molecular basis of the potential of vitamin D to prevent cancer. *Curr Med Res Opin*. 2008;24(1):139-149.

119. Holick MF, Frommer JE, McNeill SC, Richtand NM, Henley JW, Potts JT,Jr. Photometabolism of 7-dehydrocholesterol to previtamin D_3 in skin. *Biochem Biophys Res Commun*. 1977;76(1):107-114.

120. Hollis BW. Circulating 25-hydroxyvitamin D levels indicative of vitamin D sufficiency: Implications for establishing a new effective dietary intake recommendation for vitamin D. *J Nutr*. 2005;135(2):317-322.

121. Perissi V, Rosenfeld MG. Controlling nuclear receptors: The circular logic of cofactor cycles. *Nat Rev Mol Cell Biol*. 2005;6(7):542-554.

122. Gynther P, Toropainen S, Matilainen JM, Seuter S, Carlberg C, Vaisanen S. Mechanism of 1alpha,25-dihydroxyvitamin D_3-dependent repression of interleukin-12B. *Biochim Biophys Acta*. 2011;1813(5):810-818.

123. Matilainen JM, Husso T, Toropainen S, et al. Primary effect of 1alpha,25$(OH)_2D_3$ on IL-10 expression in monocytes is short-term down-regulation. *Biochim Biophys Acta*. 2010;1803(11):1276-1286.

124. Gibcus JH, Dekker J. The hierarchy of the 3D genome. *Mol Cell*. 2013;49(5):773-782.

125. Fullwood MJ, Liu MH, Pan YF, et al. An oestrogen-receptor-alpha-bound human chromatin interactome. *Nature*. 2009;462(7269):58-64.

126. Haussler MR, Haussler CA, Bartik L, et al. Vitamin D receptor: Molecular signaling and actions of nutritional ligands in disease prevention. *Nutr Rev*. 2008;66(10 Suppl 2):S98-112.

127. Pike JW, Meyer MB, Watanuki M, et al. Perspectives on mechanisms of gene regulation by 1,25-dihydroxyvitamin D_3 and its receptor. *J Steroid Biochem Mol Biol*. 2007;103(3-5):389-395.

128. Carlberg C, Seuter S. Dynamics of nuclear receptor target gene regulation. *Chromosoma*. 2010;119(5):479-484.

129. Razin A. CpG methylation, chromatin structure and gene silencing-a three-way connection. *EMBO J*. 1998;17(17):4905-4908.

X Curriculum Vitae

Personal information

Name:	Julia Wilfinger
Nationality:	Austria

Education

since November 2011	Master Nutritional Science, Molecular Nutrition University of Vienna
since October 2009	Bachelor Equine Science, University of Veterinary Medicine Vienna
from 2007 to 2011	Bachelor Nutritional Science, University of Vienna (completed with Bakk.rer.nat)
June 2007	School-leaving exam “Bundesbildungsanstalt für Kindergartenpädagogik Hartberg”, Junior high school, Qualification as a kindergarten teacher
from 1998 to 2002	Rieger Hauptschule Hartberg” Secondary modern school with focus on EDV/computers

Publications

2014	Wilfinger J, Seuter S, Tuomainen T. P, Virtanen J. K, Voutilainen S. Nurmi T, de Mello V. D. F, Uusitupa M, Carlberg C. Primary vitamin D receptor target genes as biomarkers for the vitamin D_3 status in the hematopoietic system. The Journal of Nutritional Biochemistry. 2014.

Practical trainings

2013	Internship as a research assistant in the research group of Prof. Carsten Carlberg in the laboratory at the University of Eastern Finland, Kuopio

Personal skills

Languages:	German (mother tongue) English (B2, advanced user)
Foreign experience:	ERASMUS exchange January until December 2013 in Kuopio, Finland